HI-Weak Lensing 2-Point Statistics, Synergies and Challenges

Anut Sangka in cooperation with ICG, NARIT and MeerKAT

Outline

- 21 CM line
- HI Chronology
- LSS from inhomogeneity
- Fermat Principle
- Gravitational Lensing
- Weak Gravitational Lensing
- Intensity Mapping (IM) technique
- IM challenge
- S/N and strategy
- KiDs DR4
- MeerKAT Pilot surveys
- Future

21 CM Cosmology

Hydrogen is the most abundant element in the intergalactic medium!!

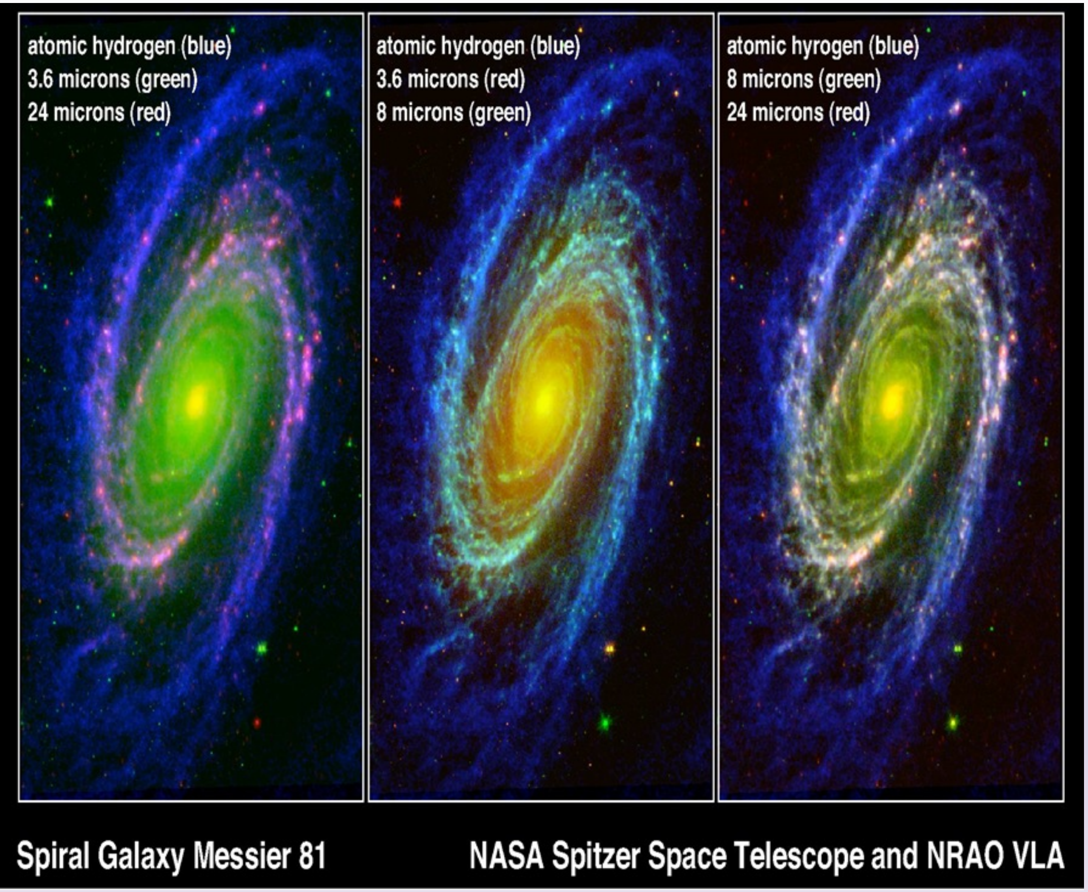

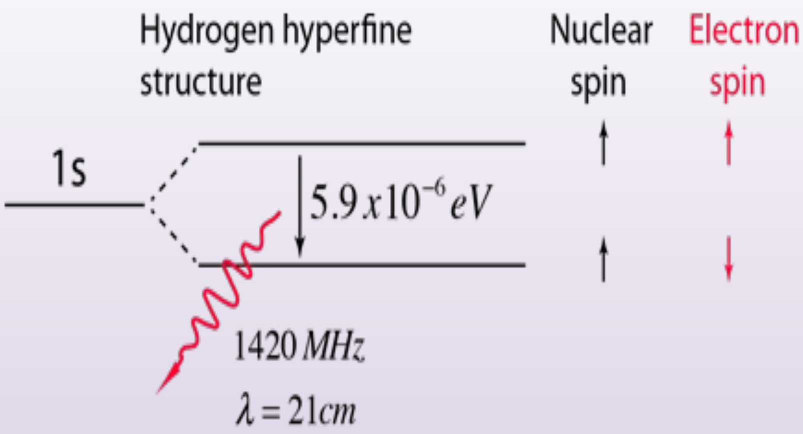

Credit: http://hyperphysics.phy-astr.gsu.edu/hbase/quantum/h21.html

HI Chronology: Early Universe

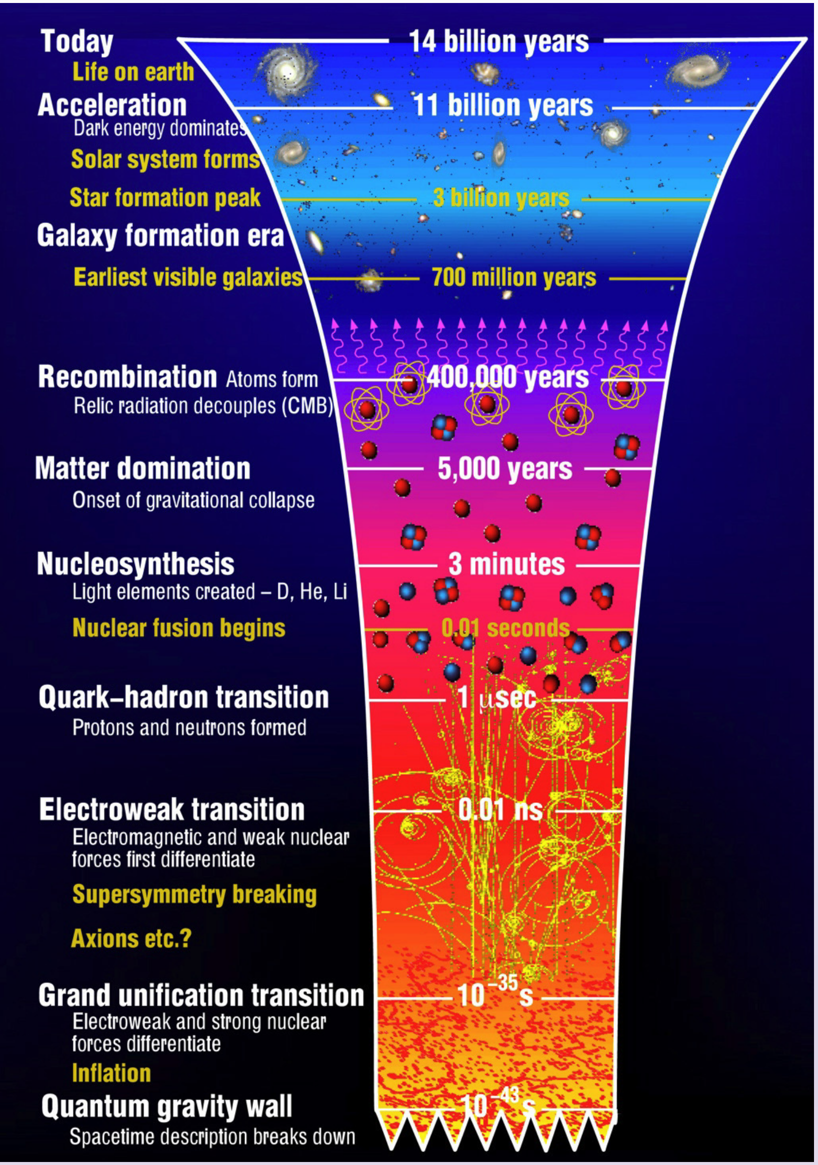

Retrieved from: https://www.ctc.cam.ac.uk/outreach/origins/big_bang_three.php

$$\varepsilon \propto a(t)^{-3(1+w)} \qquad \Omega(t) \equiv \frac{8\pi G}{3H^2(t)}\varepsilon(t)$$

$$\varepsilon = \varepsilon_{\mathrm{m}} + \varepsilon_\gamma + \varepsilon_\Lambda \qquad \Omega^{(0)} = \Omega^{(0)}_{\mathrm{m}} + \Omega^{(0)}_\gamma + \Omega^{(0)}_\Lambda$$

- **BigBang/Inflation (*t*=0):** Shortly after inflation, the Protons and Neutrons formed, technically 1st Hydrogen-1 (Prothium) isotope were formed during this time.
- **Nucleosynthesis (10s < *t* < 10^3s):** Light elements created e.g, D, He, Li, but due to high *T* and high density the universe remained ionised.
- **Matter-Radiation Equality (*t*~10^{12}s):** The densities of matter and radiation were equally. The matter components began to dominate. However, the universe was still too hot to form neutral elements.
- **Decoupling/Recombination (*t*~10^{13}s):** *z*~1100, *T*~4000K, photons were decoupling from matter. The earliest comic radiations we can directly observed (CMB). The 1st HI was formed in this era.

HI Chronology: Dark Ages and Reionisations

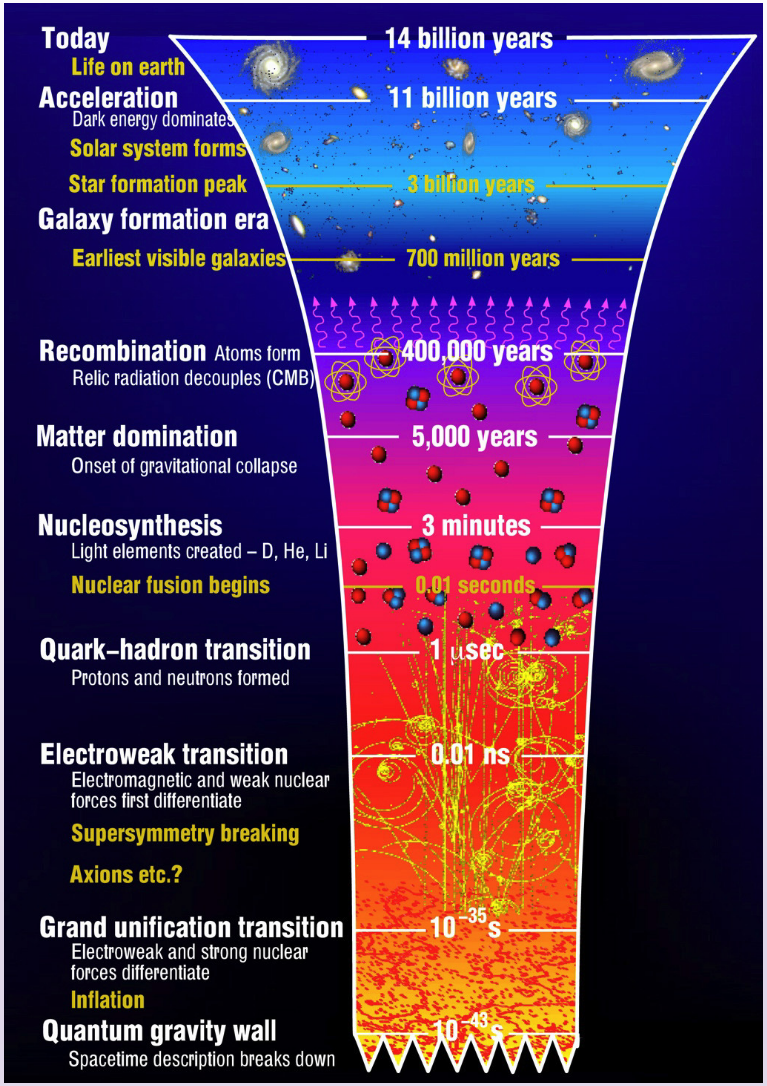

Retrieved from:

https://www.ctc.cam.ac.uk/outreach/origins/big_bang_three.php

- **The Dark Ages:** began after the HI atoms were formed. During this era the amount of HI relatively unchanged. Stars & galaxies has not yet formed. Hence, HI signal from 21cm line is an essential probe to study this era.
- **Epoch of Reionisation (EoR):** When the 1st light from star formation shined the EoR began. The first stars and galaxies were emitting UV that ionised the neutral hydrogen (HII) in the intergalactic medium (IGM). Significant pockets of HI however, persisted in the IGM. The exact time (redshift) of this period is still a subject to be discussed.

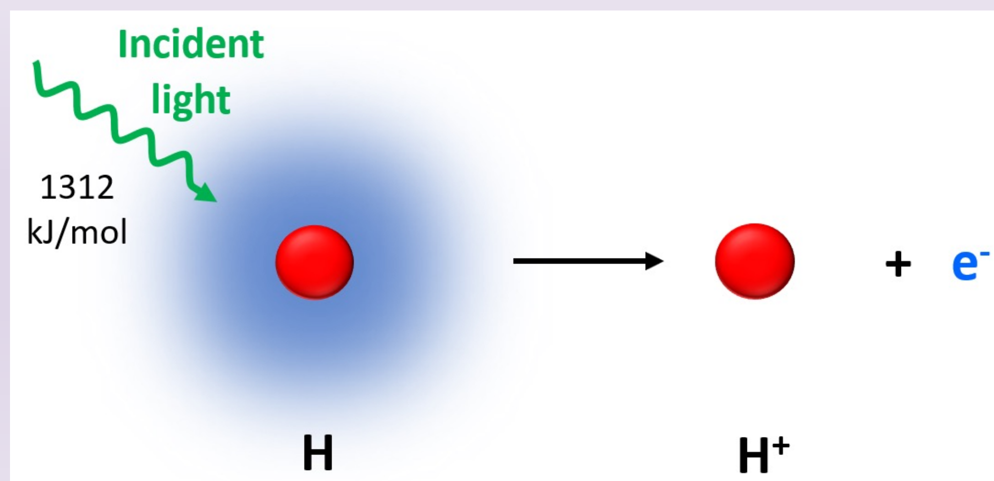

HI Chronology: Post EoR

- Only HI in dense regions of galaxies could survived the ionisation process while the universes kept expanding.
- Allowing us to consider HI as a bias tracer to Large Scale Structure (LSS).
- Due to difficulty in 21cm signal detection, we cannot safely state that the chance to detect HI outside galaxy is zero.
- However, late-time HI via computer simulations suggest that majority of post-reionisation HI resides within DM Halo

$$\delta_{\mathrm{HI}} = b_{\mathrm{HI}} \delta_{\mathrm{m}}$$ (Late-time only)

Why ? Have a discussion with your partners

The Inhomogeneous Universe

- Cosmological Principle is a linear approximation for large scale.
- However, LSS can be formed due to inhomogeneity.
- The (Newtonian limit) line element of perturbed RW metric is

$$ds^2 = -\left(1 + \frac{2\Phi}{c^2}\right)c^2 dt^2 + a^2(t)\left(1 - \frac{2\Phi}{c^2}\right)[d\chi^2 + \chi^2(d\theta^2 + \sin^2\theta d\phi^2)],$$

where $\nabla_\chi^2 \Phi = \frac{3\Omega_\mathrm{m}}{2H_0 a}\delta(a)$ and $\delta = \frac{\rho - \bar{\rho}}{\bar{\rho}}$.

- Linear perturbation theory leads to

$$\ddot{\delta} + 2\frac{\dot{a}}{a}\dot{\delta} = 4\pi G\rho_0\delta,$$

$\delta(\boldsymbol{\chi}, t) = D_\pm(t)\delta(\boldsymbol{\chi})$ (Flat, matter dominanted universe)

Inhomogeneous Universe Part 2

$$D_+(t) \propto a(t) \propto t^{2/3} \quad \text{and} \quad D_-(t) \propto t^{-1}$$

We can also approximate density perturbation such that,

$$\delta(a) \propto a \frac{\delta(\Omega_\mathrm{m}, \Omega_\Lambda)}{\delta(\Omega_\mathrm{m} = 1)} = a f[\Omega_\mathrm{m}(a)],$$

$$f[\Omega_\mathrm{m}(a)] \simeq \frac{5}{2}\Omega_\mathrm{m}\left[\Omega_\mathrm{m}^{4/7} - \Omega_\Lambda + \left(1 + \frac{1}{2}\Omega_\mathrm{m}\right)\left(1 + \frac{1}{70}\Omega_\Lambda\right)\right]^{-1}$$

Carroll et al (1992)

For flat LCDM:

$$f[\Omega_\mathrm{m}(a)] \simeq \Omega_\mathrm{m}^{2.3}$$

Fermat Principle

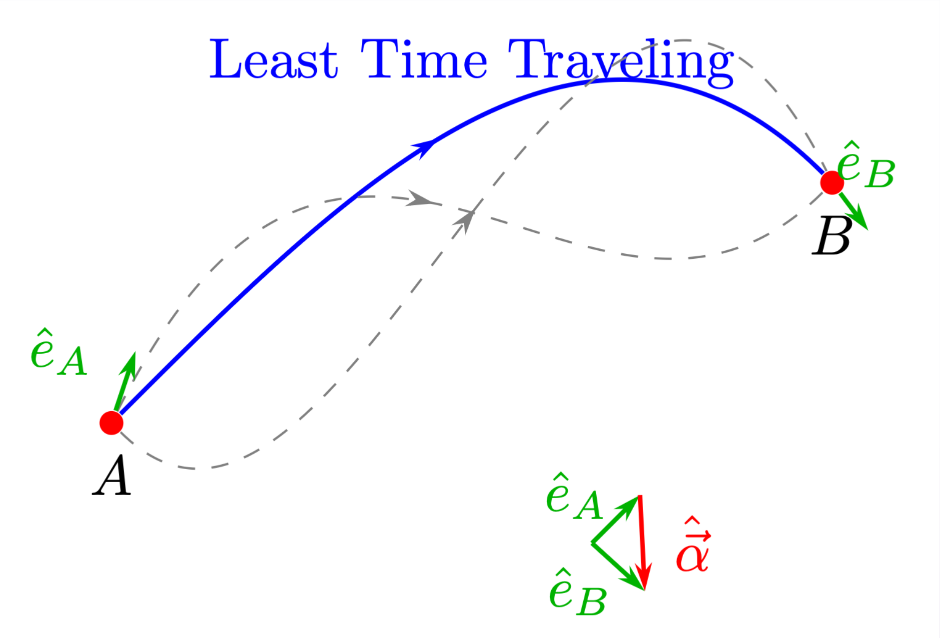

The path a ray takes between two points is such that the time taken to traverse the distance is shortest, longest or stationary in relation to nearby rays.

$$t = \frac{1}{c}\int_A^B n(\mathbf{x})dl$$

$$dl = \left[\left(\frac{\partial x}{\partial l}\right)^2 + \left(\frac{\partial y}{\partial l}\right)^2 + \left(\frac{\partial z}{\partial l}\right)^2\right]^{1/2} dl$$

Fermat Principle: Part II

Let

$$f(\mathbf{x},\mathbf{x}') = n(\mathbf{x})[x'^2 + y'^2 + z'^2]^{1/2} \quad \text{where} \quad x' := \frac{\partial x}{\partial l}\ y' := \frac{\partial y}{\partial l} \text{ and } z' := \frac{\partial z}{\partial l}$$

Now we can write down an interval *t* as:

$$ct = \int_A^B f(\mathbf{x},\mathbf{x}')dl$$

Varying this integral from $\mathbf{x} \rightarrow \mathbf{x} + \delta\mathbf{x}$ and $t \rightarrow t + \delta t$, we obtain

$$\begin{aligned} \delta t &= \frac{1}{c}\int_A^B \left(\frac{\partial f}{\partial x_i}\delta x_i + \frac{\partial f}{\partial x_i'}(\partial x_i)'\right)dl, \\ &= \frac{1}{c}\int_A^B \left(\frac{\partial f}{\partial x_i} - \frac{d}{dl}\frac{\partial f}{\partial x_i'}\right)\delta x_i dl + \left[\frac{\partial f}{\partial x_i'}\delta x_i\right]_A^B, \end{aligned}$$

where we apply integration by part to the integral get the second integration.

As δx_i must be stationary at the end-points A and B, hence the second term must be vanished. The Fermat principle states that $\delta t = 0$, therefore

$$\frac{\partial f}{\partial x_i} - \frac{d}{dl}\frac{\partial f}{\partial x'} = 0$$

Varying Reflection Index

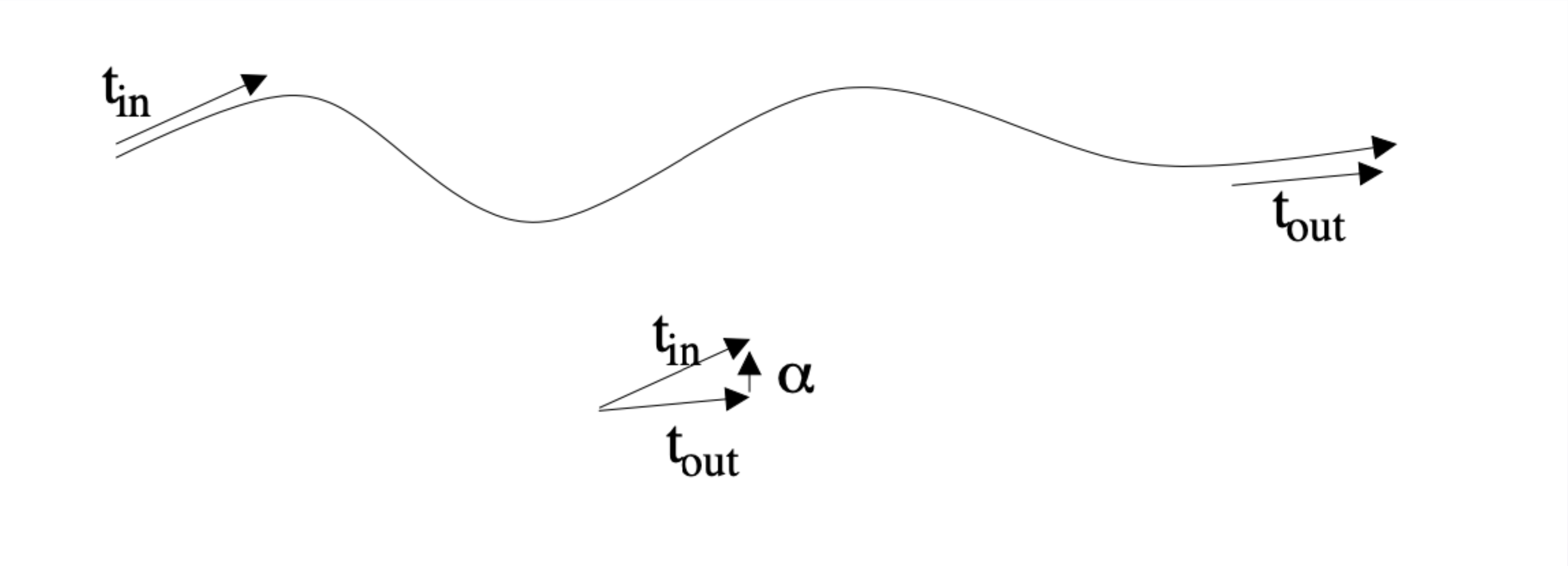

$$\mathbf{t}(l) = \frac{dx^a(l)}{dl}\mathbf{e}_a,$$

$$\hat{\vec{\alpha}} = \mathbf{t}_{\text{in}} - \mathbf{t}_{\text{out}},$$

$$\hat{\vec{\alpha}} = -\int dl \frac{d\mathbf{t}}{dl},$$

Using Euler's Equation ➡️

Deflection vector

$$\hat{\vec{\alpha}} = -\int dl \frac{\nabla_\perp n}{n}.$$

Gravitational Lensing

$$ds^2 = -\left(1+\frac{2\Phi}{c^2}\right)c^2dt^2 + a^2(t)\left(1-\frac{2\Phi}{c^2}\right)[d\chi^2+\chi^2(d\theta^2+\sin^2\theta d\phi^2)],$$

$$ds^2 = 0 \quad \text{for} \quad \text{light ray}$$

$$\text{let } ad\eta = dt \text{ then } d\eta \to dt'$$

$$d\chi \to dl$$

$$ct = \int \left(1-\frac{2\Phi}{c^2}\right)^{1/2}\left(1+\frac{2\Phi}{c^2}\right)^{-1/2} dl \;\simeq \int dl\left(1-\frac{2\Phi}{c^2}\right)$$

Gravitationally refractive index

$$\boxed{n = 1 - \frac{2\Phi}{c^2}}$$

Deflection angle

$$\boxed{\hat{\vec{\alpha}} = \frac{2}{c^2}\int dl \nabla_\perp \Phi}$$

Modified Gravity

A modification of GR or an anisotropic stress pressure perturbation have a line element such that

$$ds^2 = -\left(1 + \frac{2\Psi}{c^2}\right)dt^2 + \left(1 - \frac{2\Phi}{c^2}\right)dl^2$$

This leads to a deflection angle

$$\hat{\vec{\alpha}} = \frac{1}{c^2}\int \nabla_\perp(\Phi + \Psi)dl$$

In the late-time universe the anisotropy in stress-pressure is minimal and can be neglected. So, we can detect the modification of GR via lensing,

Lens Effect

$$\hat{\vec{\alpha}} = \frac{2}{c^2} \int dl \nabla_\perp \Phi$$

Born Approximation

$$\hat{\vec{\alpha}}(\hat{n}) \simeq \frac{2}{c^2} \int d\chi \nabla_{\perp \mathrm{com}} \Phi(\chi, \hat{n})$$

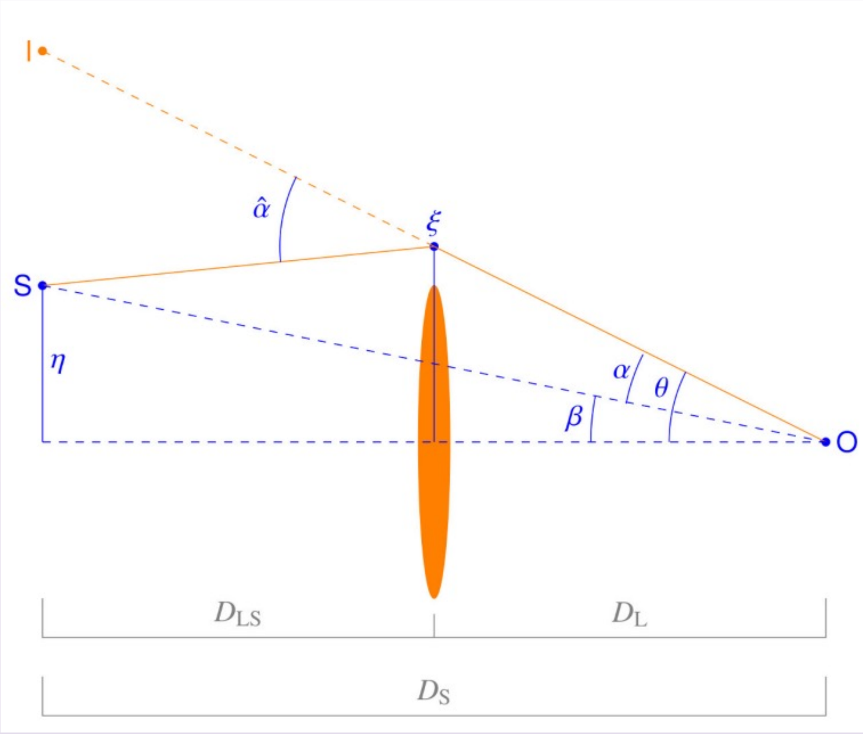

Bertelmann & Maturi 2017

Point Mass Lensing

$$\hat{\vec{\alpha}} = \frac{4GM}{c^2 \xi}$$

$$\vec{\theta} D_s = \vec{\beta} D_s + \hat{\vec{\alpha}} D_{ls}$$

$$\boxed{\vec{\alpha} = \frac{D_{ls}}{D_s} \hat{\vec{\alpha}}}$$

$$\boxed{\vec{\theta} = \vec{\beta} + \vec{\alpha}}$$

Lensing Potential

$$\psi = \frac{2D_{ls}}{c^2 D_s D_l} \int \Phi(D,\theta) dD \quad \text{where } d\chi = dD/a$$

$$\vec{\alpha} = \nabla_\theta \psi \qquad \nabla_\theta = \left(\frac{\partial}{\partial \theta_x}, \frac{\partial}{\partial \theta_y} \right)$$

Take Divergence

$$\nabla_\theta \cdot \vec{\alpha} = \nabla^2 \theta \psi = \frac{2}{c^2} \frac{D_l D_{ls}}{D_s} \int \nabla_\perp^2 \Phi(D,\theta) dD$$

Poisson Equation:

$$\nabla^2 \Phi = 4\pi G \rho$$

$$\nabla_\theta^2 \psi = 2\kappa = 2\frac{\Sigma}{\Sigma_\mathrm{c}}$$

$$\Sigma := \int dD \rho(D,\theta) \quad \text{and} \quad \Sigma_\mathrm{c} := \frac{c^2}{4\pi G} \frac{D_s}{D_l D_{ls}}$$

Jacobian and Distortion of Image

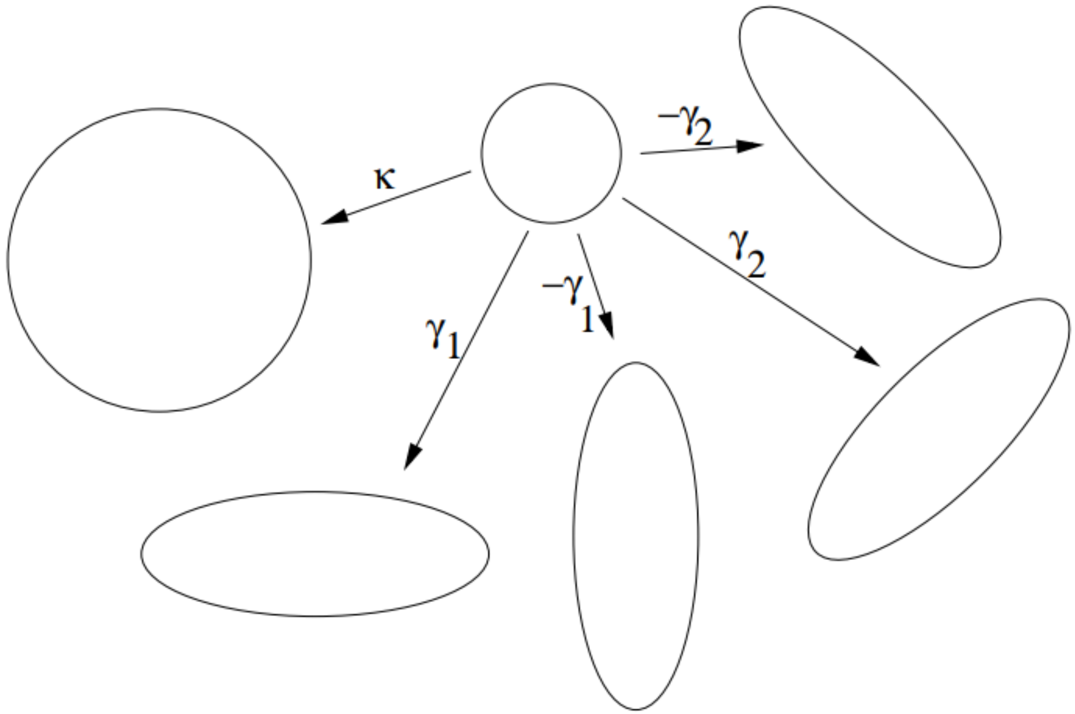

$$\mathcal{A}_{ij} = \frac{\partial \beta_i}{\partial \theta_j} = \delta_{ij} - \frac{\partial \psi}{\partial \theta_i \partial \theta_j} = \delta_{ij} - \psi_{ij}$$

$$\mathcal{A} = \begin{pmatrix} 1-\kappa-\gamma_1 & -\gamma_2 \\ -\gamma_2 & 1-\kappa+\gamma_1 \end{pmatrix} = (1-\kappa)\begin{pmatrix} 1 & 0 \\ 0 & 1 \end{pmatrix} - \begin{pmatrix} \gamma_1 & \gamma_2 \\ \gamma_2 & -\gamma_1 \end{pmatrix}.$$

Distortion of Image and Ray Tracing

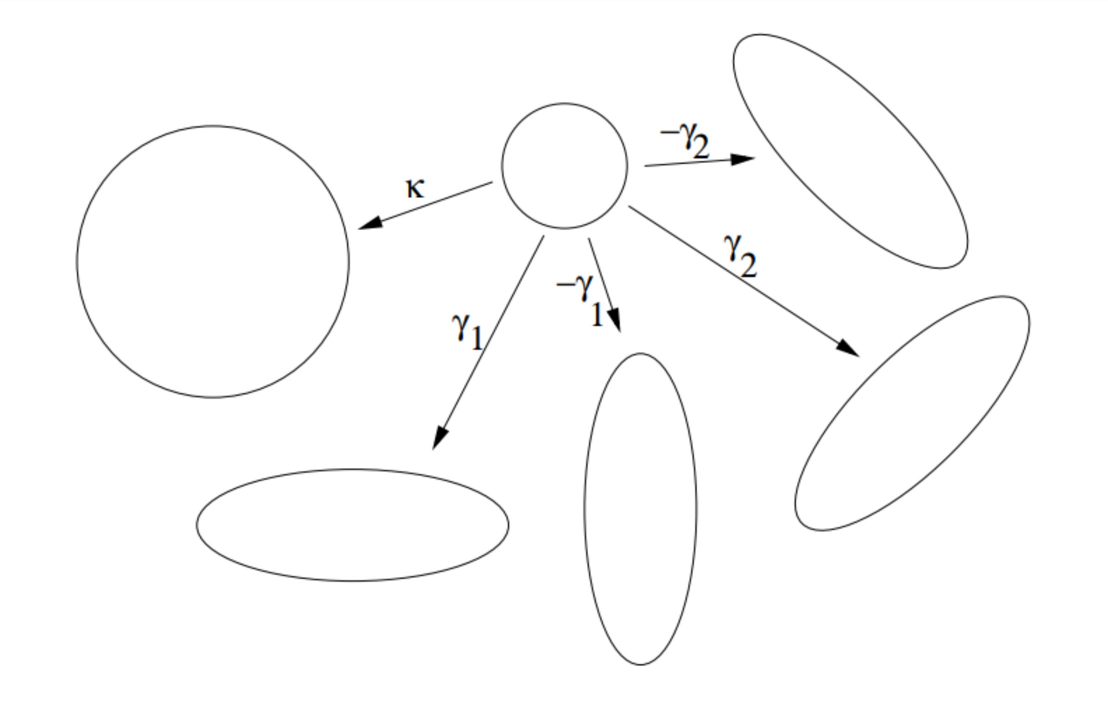

$$\gamma_1 := \frac{1}{2}(\psi_{11} - \psi_{22}),$$

$$\gamma_2 := \psi_{12}$$

$$\mu = \frac{1}{1 - (\kappa^2 - \gamma^2)} \approx 1 + 2\kappa$$

Weak Regime

Surface Brightness is conserved

$$\mathrm{I}(\theta) = \mathrm{I_s}(\beta)$$

can only be detected by measuring distortions statistically

$$\mathrm{I}(\theta_0 + \delta\theta) = \mathrm{I_s}(\beta_0 + \delta\beta) = \mathrm{I_s}(\beta_0 + \mathcal{A}\delta\theta)$$

Shear induce ellipticity of circular source

Intrinsic ellipticity variance

$$\sigma_e \simeq 0.3$$

Expectation variance ellipticity signal from N galaxies

$$\sigma_{\bar{e}} = \sigma_e/\sqrt{N}$$

To detect lensing cosmic variance signal, we require:

$$\sigma_\gamma > \sigma_{\bar{e}}$$

Measuring Shear

quadrupole moments

$$Q_{ij} = \frac{1}{F} \int \mathrm{I}(\theta)\theta_i\theta_j d^2\theta$$

Blandford & Narayan(1986); Blandford et al. (1991)

$$e_1 = \frac{Q_{11} - Q_{22}}{Q_{11} + Q_{22}} \quad e_2 = \frac{2Q_{12}}{Q_{11} + Q_{22}}$$

Measuring ellipticity is equivalent to mearing shear

$$\gamma_\alpha \simeq \frac{e_\alpha}{2 - \sigma_e^2}$$

$\gamma \simeq \langle e \rangle \simeq \langle e_\alpha \rangle / 2$ Quiz Why ?

HW

$$\mathrm{I}(\theta_0 + \delta\theta) = \mathrm{I_s}(\beta_0 + \delta\beta) = \mathrm{I_s}(\beta_0 + \mathcal{A}\delta\theta)$$

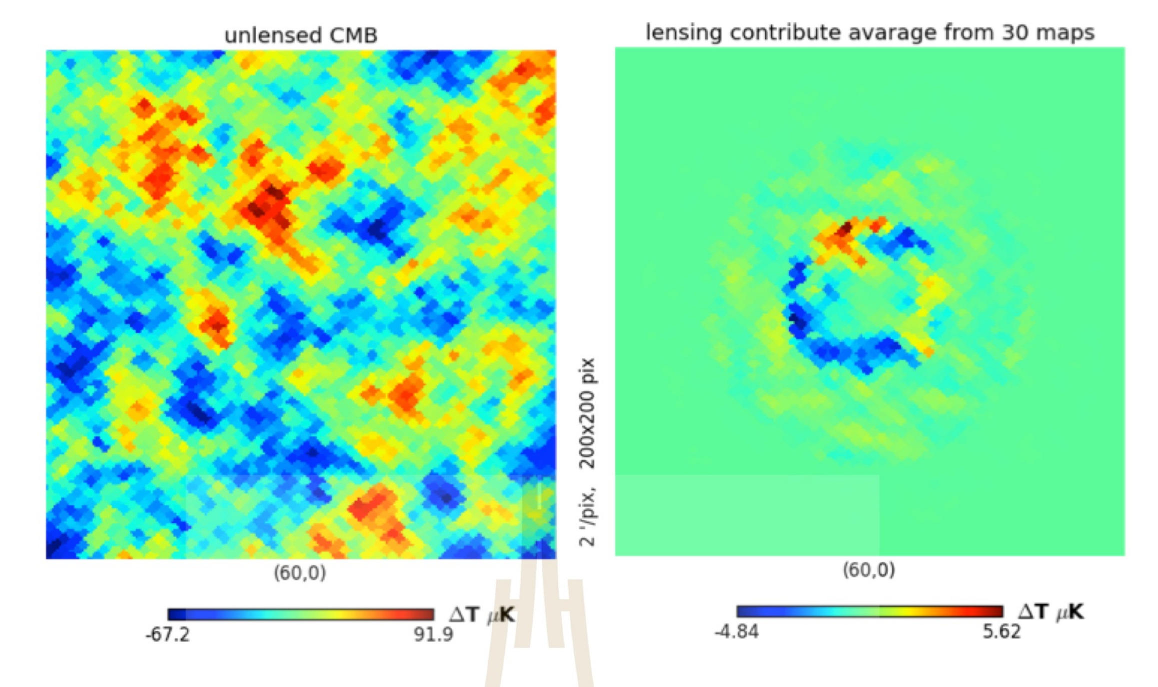

Point Source lensing

$$\hat{\vec{\alpha}} = \frac{4GM}{c^2\xi}$$

$$\vec{\theta}D_s = \vec{\beta}D_s + \hat{\vec{\alpha}}D_{ls}$$

$$\boxed{\vec{\alpha} = \frac{D_{ls}}{D_s}\hat{\vec{\alpha}}}$$

$$\boxed{\vec{\theta} = \vec{\beta} + \vec{\alpha}}$$

Use these equation to create a lensed image

Hint: 2nd order Taylor's expansion

Write your lens equation

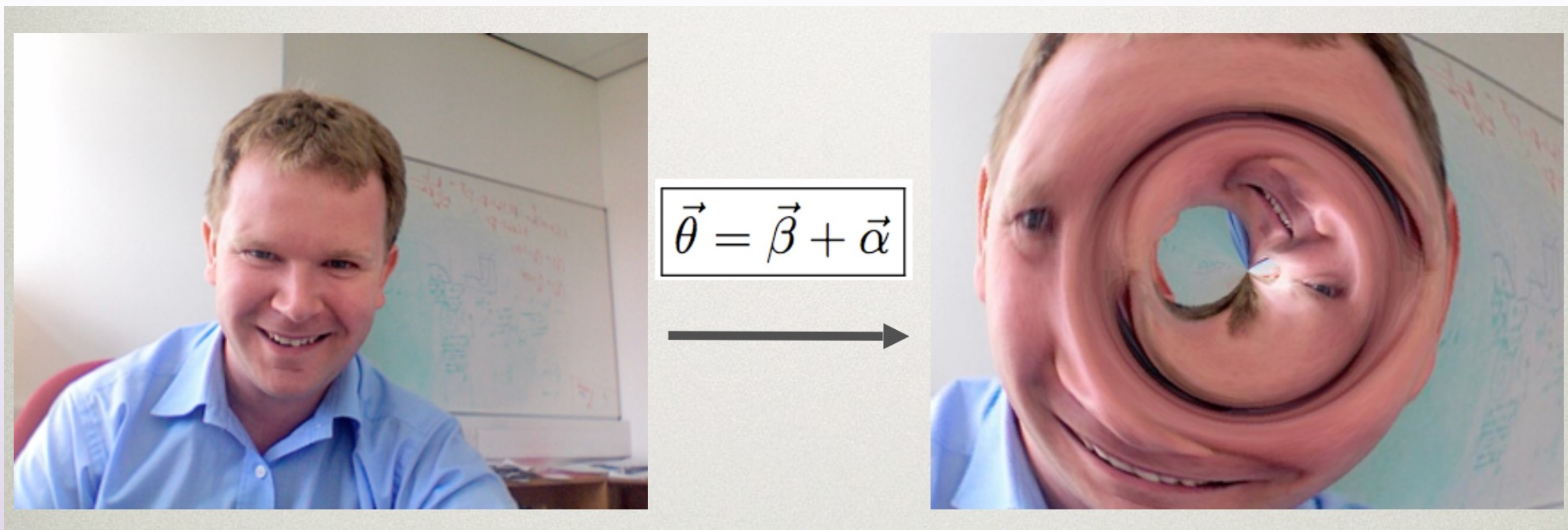

Lensing Kernel

- Deflection angle

$$\alpha(\hat{n}) = \int_0^{\chi_s} d\chi' q_L(\chi', \chi_s) \nabla_\perp \phi_W(\chi', \chi' \hat{n})$$

Lensing kernel

$$q_L(\chi', \chi_s) = \frac{\chi'(\chi_s - \chi')}{\chi_s}$$

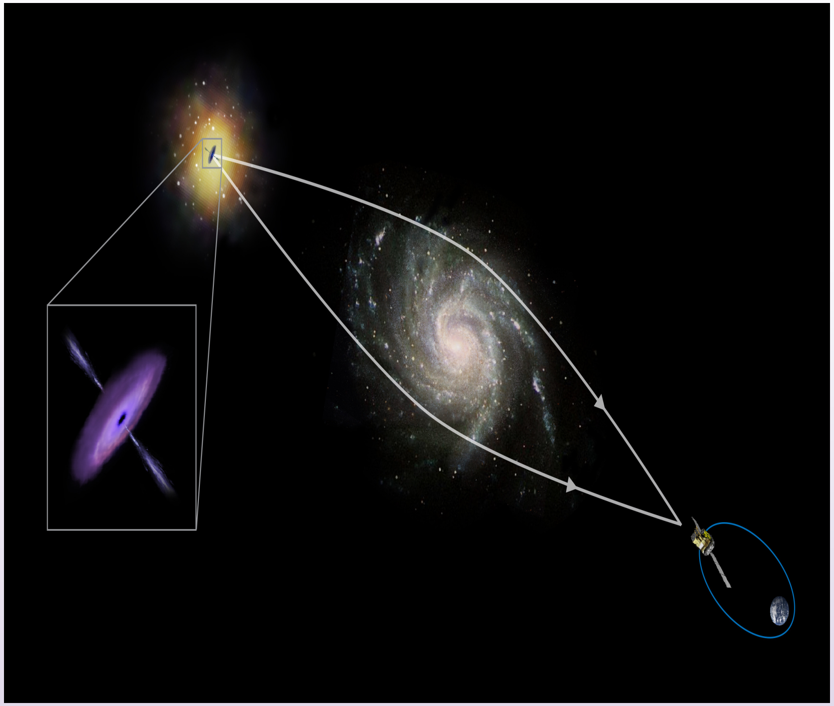

Back to HI: Intensity mapping technique

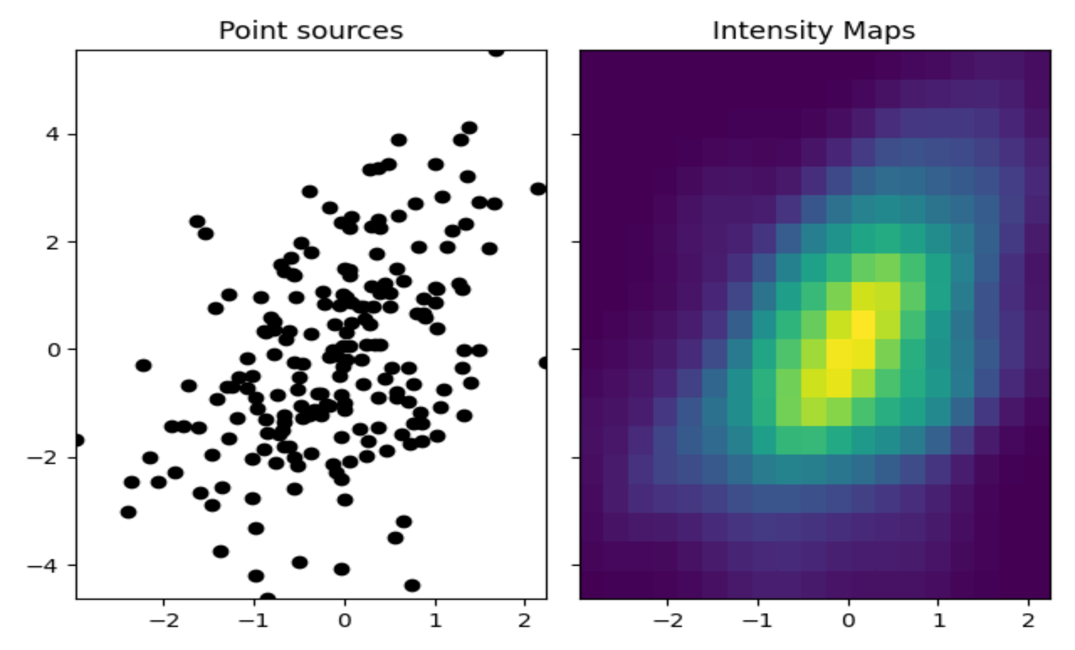

$$\Delta T_{\rm HI}(z,\hat{n}) = \bar{T}_{\rm HI}(z) b_{\rm HI}(z) \delta(z,\hat{n})$$

$$\bar{T}_{\rm HI}(z) = 180 \Omega_{\rm HI}(z) h \frac{(1+z)^2}{H(z)/H_0} [\mathrm{mK}]$$

Battye et al. (2013)

$$\Omega_{\rm HI}(z) = 0.00048 + 0.00039z - 000065z^2$$

SKA cosmology SWG et. al 2018

$$[\Delta T_{\rm HI}(k,z)]^2 = \bar{T}_{\rm HI}(z)^2 [b_{\rm HI}(k,z)]^2 \frac{k^3 P_\delta(k,z)}{2\pi^2}$$

$$T_{\rm b}(\hat{\theta},\nu) = \left(\frac{3\hbar c^3 A_{10}}{16 k_B \nu_{21}^2} \right) \frac{x_{\rm HI} n_{\rm HI}}{(1+z)^2 (dv_{||}/dr_{||})} \left(1 - \frac{T_\gamma}{T_s} \right)$$

Lewis & Challinor, 2007

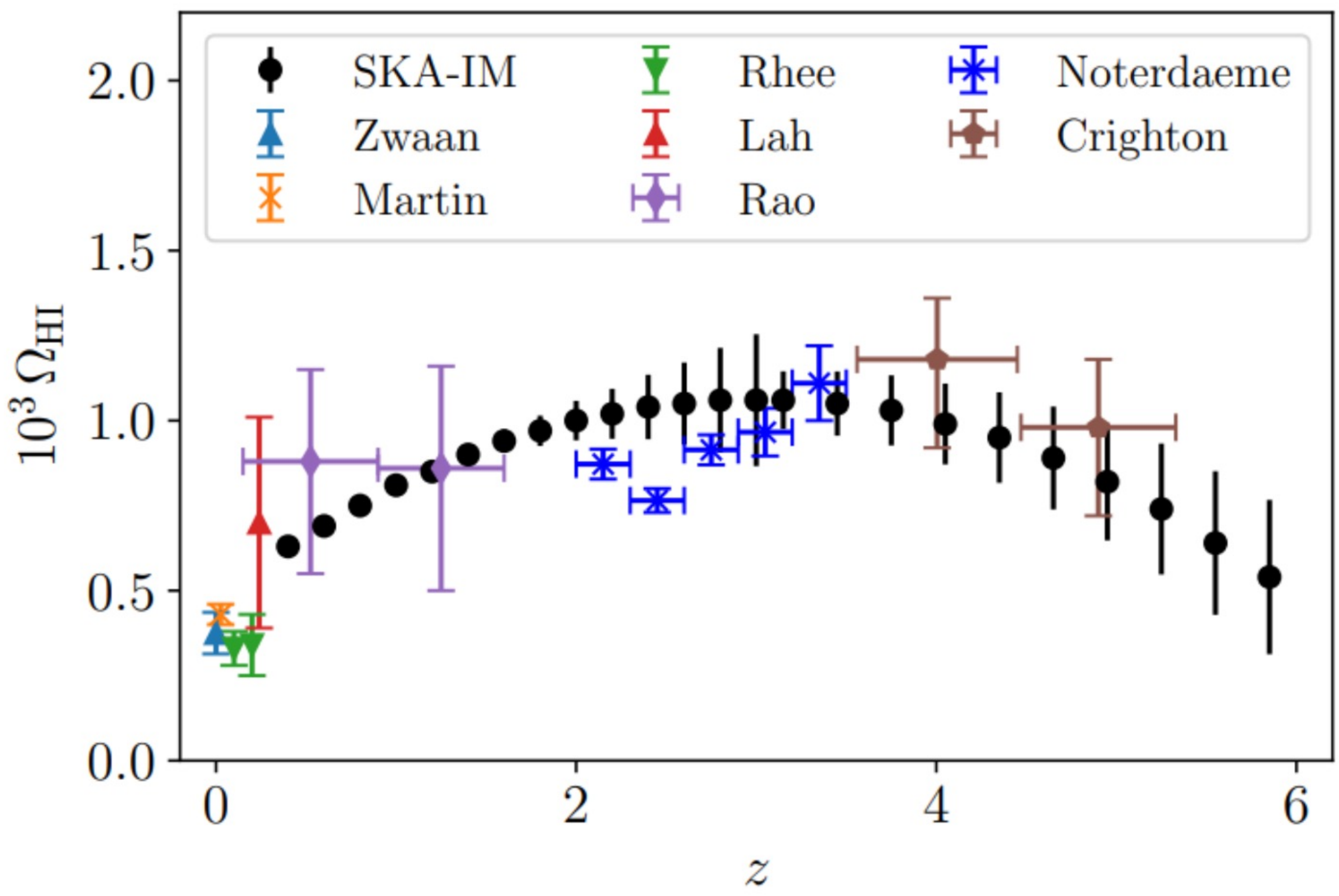

Figure 2.5: This figure shows the measurements of $\Omega_{\rm HI}$ from various surveys and the forecast for SKA-IM (black dots). The plot shows the measurements and forecasts from redshift 0 to 6, (Square Kilometre Array Cosmology Science Working Group et al., 2020).

The problem(s)

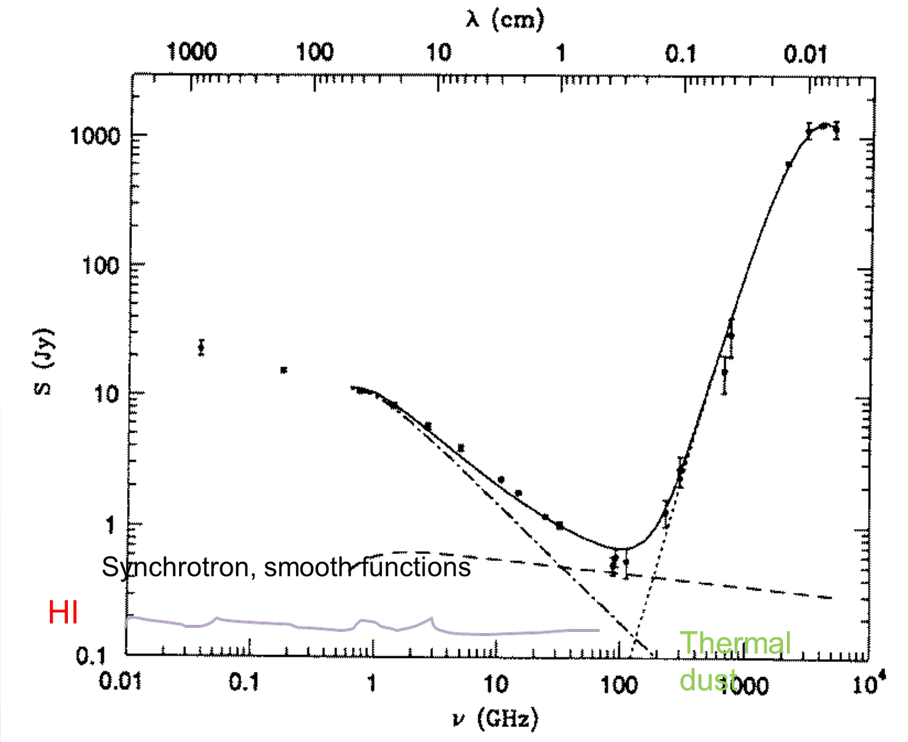

[Klein et al. 1988](), [Carlstrom & Kronberg 1991]()

$$C_\ell(\nu_1,\nu_2) = A\left(\frac{\ell_{\rm ref}}{\ell}\right)^\beta \left(\frac{\nu_{\rm ref}^2}{\nu_1\nu_2}\right)^\alpha \exp\left(-\frac{\log^2(\nu_1/\nu_2)}{2\xi^2}\right)$$

Free-Free, point source modelling

- Low signal compares to foreground, e.g.Galactic Synchrotron Radiation, which has > 3 order of magnitude brighter than HI.
- So, we apply foreground removal technique by removing the radial long wavelength modes.
- How ever this should reduce the signal in HI-lensing correlation
- Poor angular resolutions
- HI Bias

2-point functions

Spherical Harmonic

$$f(\theta,\phi)=\sum_{\ell m} a_{\ell m}Y_{\ell m}(\theta,\phi)$$

Angular power spectra

$$C_\ell^{XY} =< a_{\ell m}^{X} a_{\ell m}^{Y*} >_m$$

- small deflection angle => flat sky approximation => Limber approximation

$$C_\ell^{XY} = \int d\chi \, q^X(\chi) q^Y(\chi) P_\delta\left(\frac{\ell+1/2}{\chi}, z(\chi)\right)$$

$$q^{\rm HI}(\chi) = \bar{T}_{\rm HI}(\chi) b_{\rm HI}(\chi) \frac{n^i_{\rm HI}(z(\chi))}{\bar{n}^i_{\rm HI}} \frac{dz}{d\chi}, \quad q^\kappa(\chi) = \frac{3\Omega_m H_0^2}{2c^2}\frac{\chi}{a(\chi)}\int_\chi^\infty d\chi' \frac{n_s^i(z(\chi'))\frac{dz}{d\chi'}}{\bar{n}_s^i}\frac{\chi'-\chi}{\chi'}$$

Measuring density perturbation is equivalent to measure gravitational potential

$$\boxed{\Phi_{\ell m} = -\frac{3\Omega_{\rm m}H_0^2}{2ak^2}\delta_{\ell m}(k).}$$

$$\boxed{C_\ell(\nu_1,\nu_2) = A\left(\frac{\ell_{\rm ref}}{\ell}\right)^\beta \left(\frac{\nu_{\rm ref}^2}{\nu_1\nu_2}\right)^\alpha \exp\left(-\frac{\log^2(\nu_1/\nu_2)}{2\xi^2}\right)}$$

Multipoles Expansion

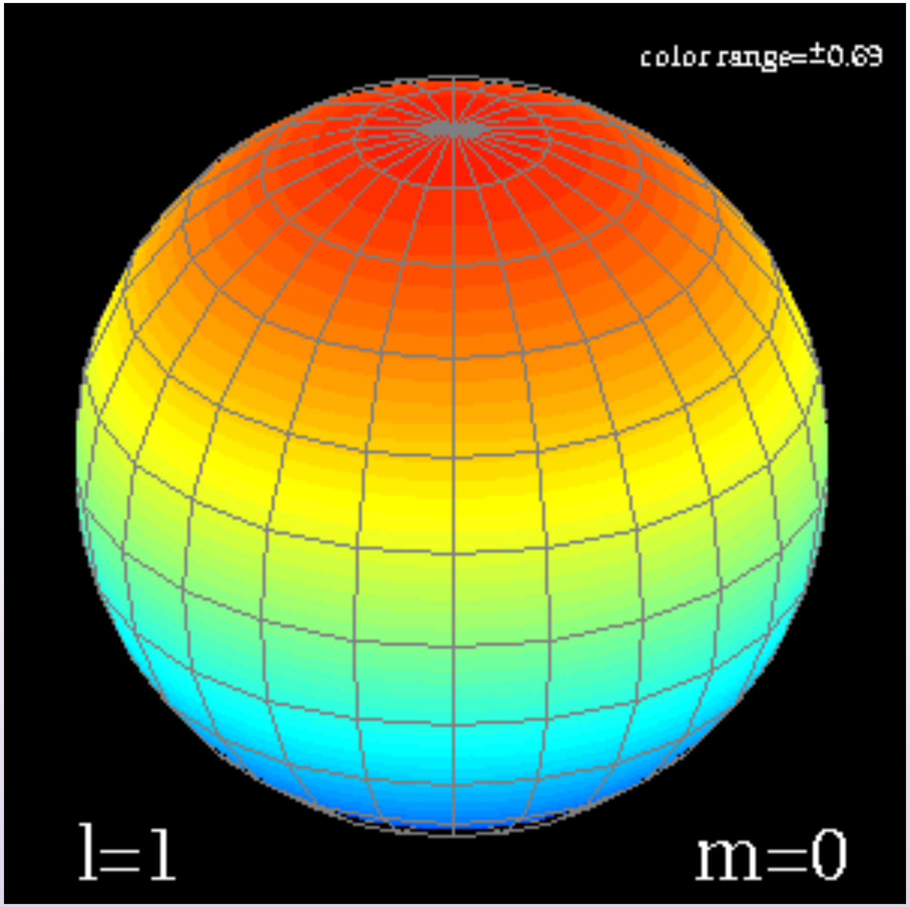

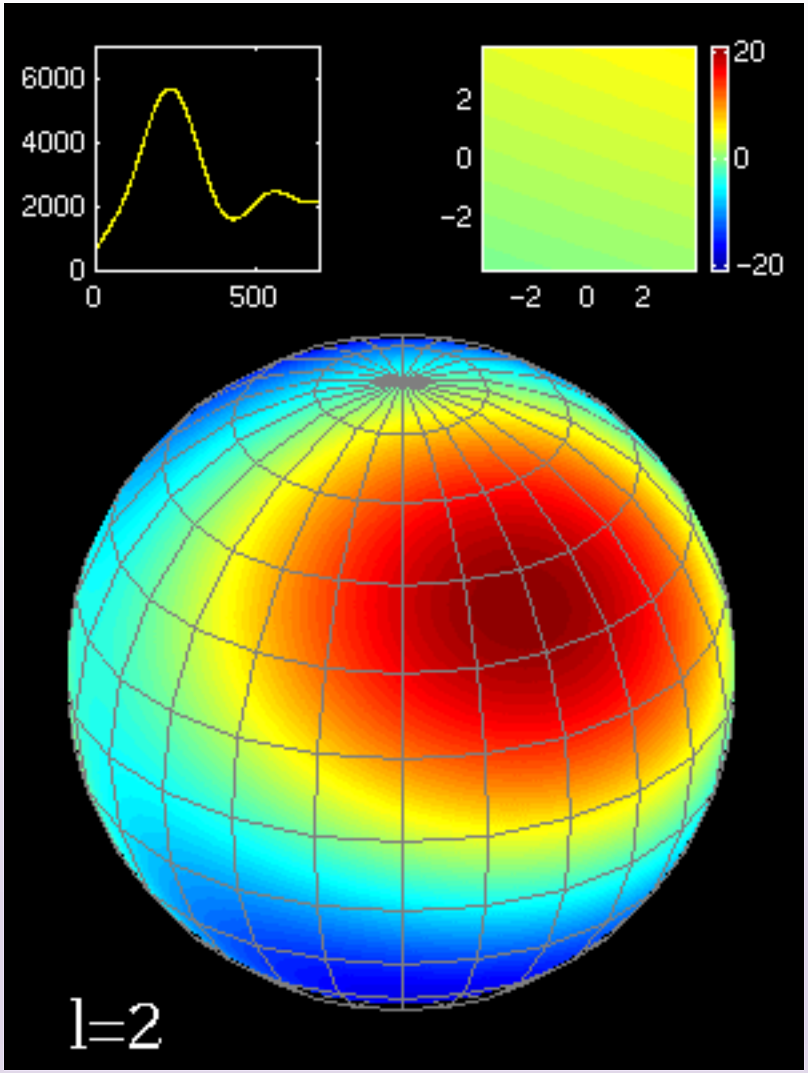

http://find.spa.umn.edu/~pryke/logbook/20000922/

N-Body Simulations

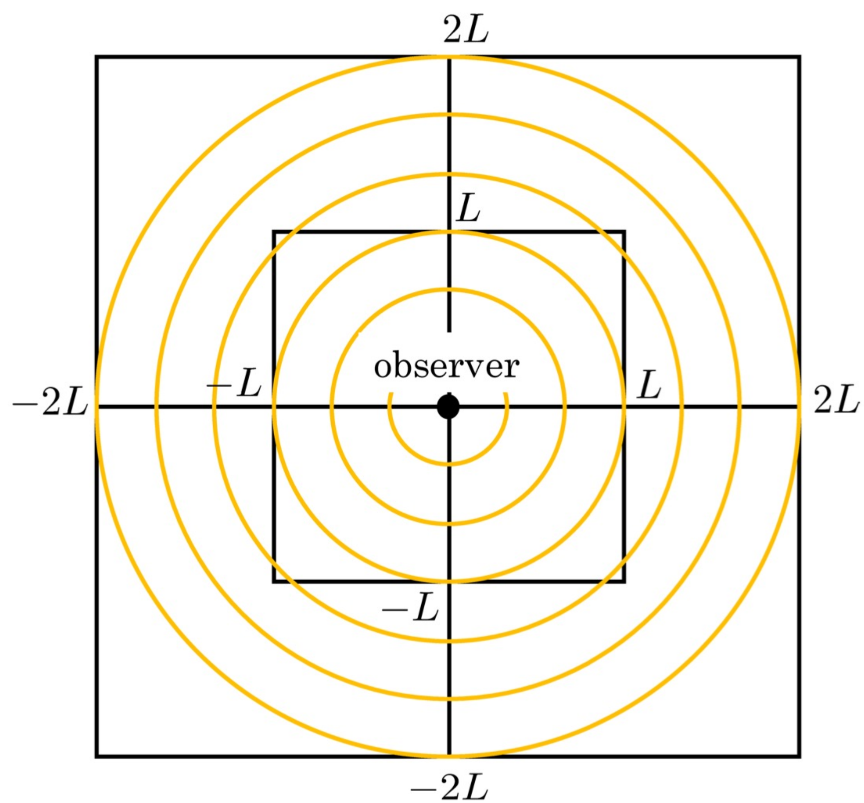

FIG. 1.— Configuration of ray-tracing simulation with cubic simulation boxes of lengths $L, 2L, 3L, \cdots$, where $L = 450\,h^{-1}$Mpc (comoving scale), placed around the observer. The figure shows the inner two boxes with side lengths L and $2L$, respectively. The observer is located at the vertex of the boxes. In each box, we constructed three spherical shells with thickness of $\Delta r = L/3 = 150\,h^{-1}$Mpc; the orange circles show the boundaries between the shells.

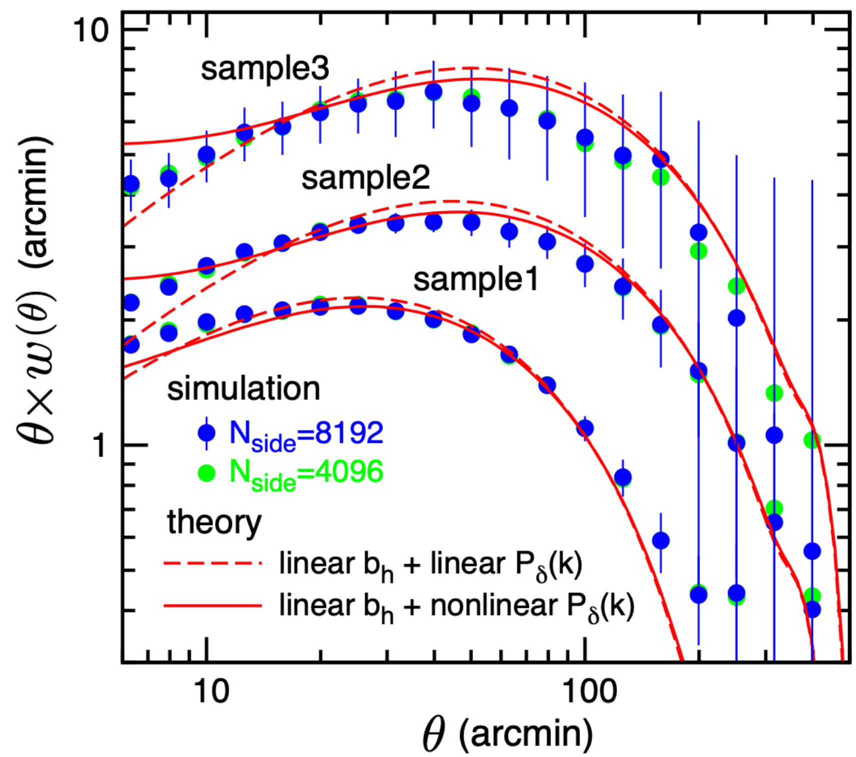

Takahashi et al 2017 1706.01472

Chalawan HPC

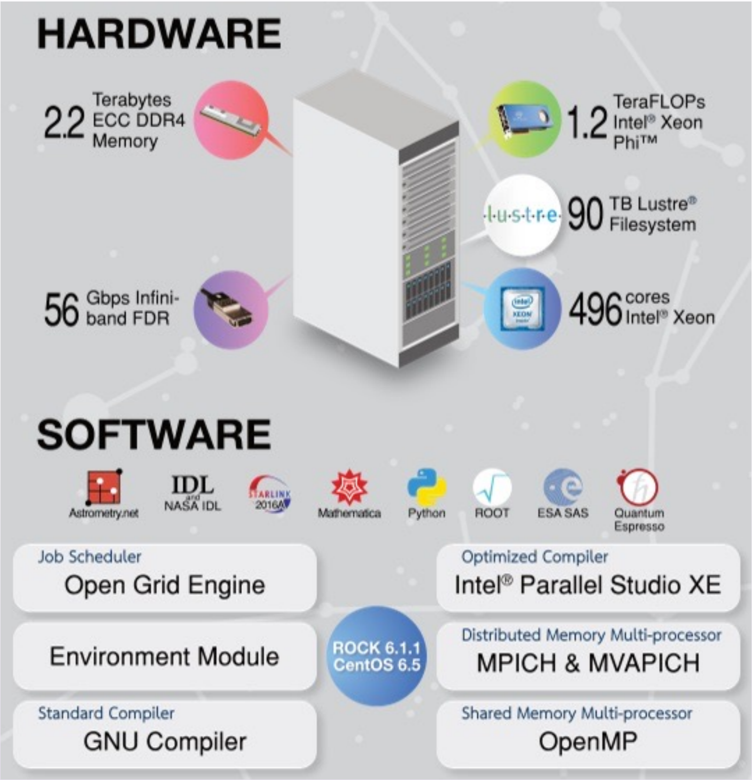

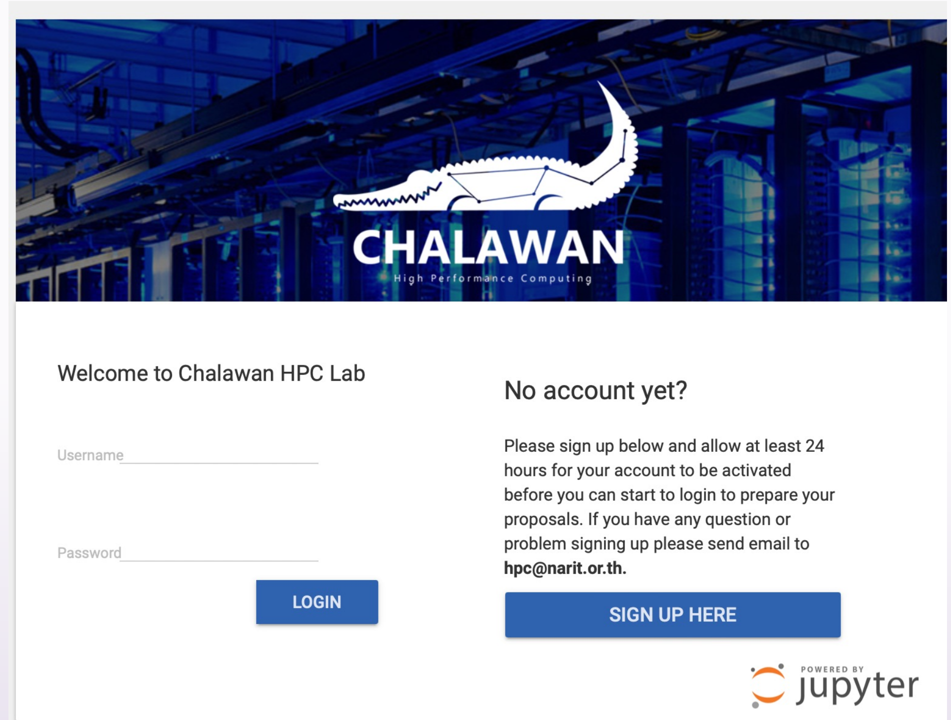

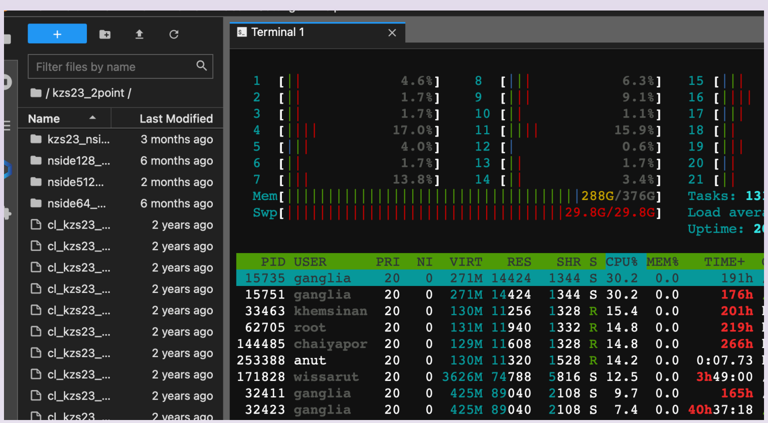

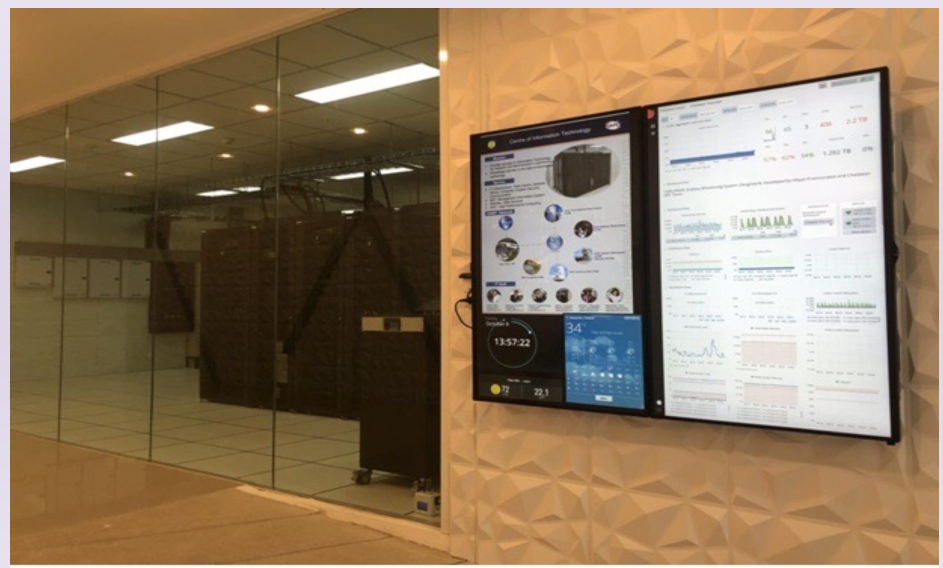

Blind Foreground Subtraction

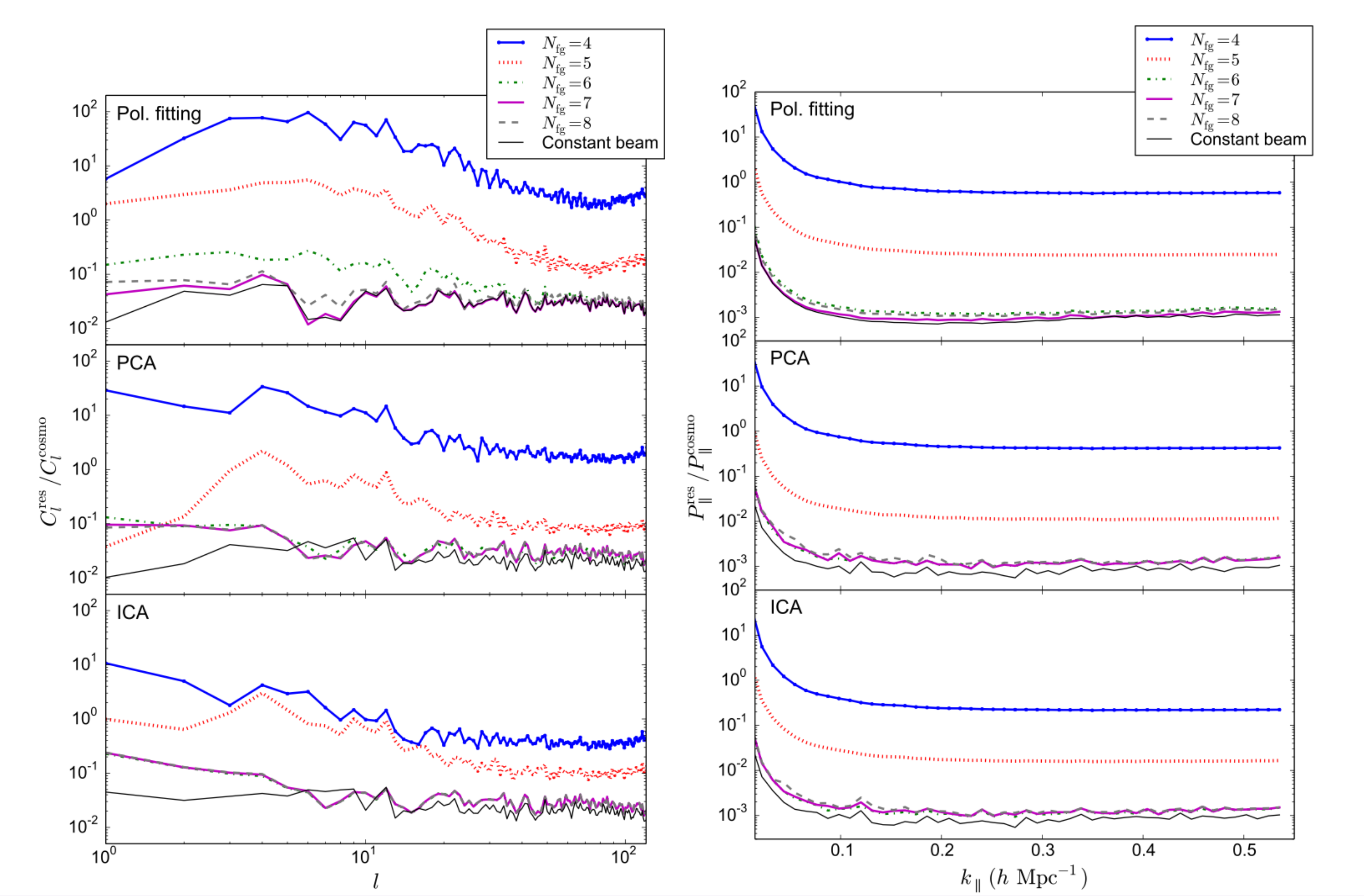

Alonso et. al 2024 https://arxiv.org/abs/1409.8667

Blind Foreground Subtraction: LoS method

$$T(\nu, \hat{\theta}) = \sum_{k=1}^{N_{fg}} f_k(\nu) S_k(\hat{n}) + T_{\rm cosmo}(\nu, \hat{n}) + T_{\rm noise}(\nu, \hat{\nu})$$

Components

$$\Delta T_{\rm HI}^{\rm clean}(\hat{n}, z) = \Delta T_{\rm HI}^{\rm orig}(\hat{n}, z) - \Delta T_{\rm HI}^{\rm LoS}(\hat{n})$$

Equivalent to long wavelength mode in radial direction

$$\Delta T_{\rm HI}^{\rm LoS}(\hat{n}) = \frac{1}{N_z} \sum_i \bar{T}_{\rm HI}(z_i) b_{\rm HI}(z_i) \delta(\hat{n}, z_i)$$

icg Portsmouth

Mock Catalogues & Simulations

- Takahashi et al. 2017, based on 9 years WMAP
- 35 of 107 realisations are selected,
- Catalogues provides lensing convergence, using the density profile to generate HI.

Uncleaned Cleaned Residue

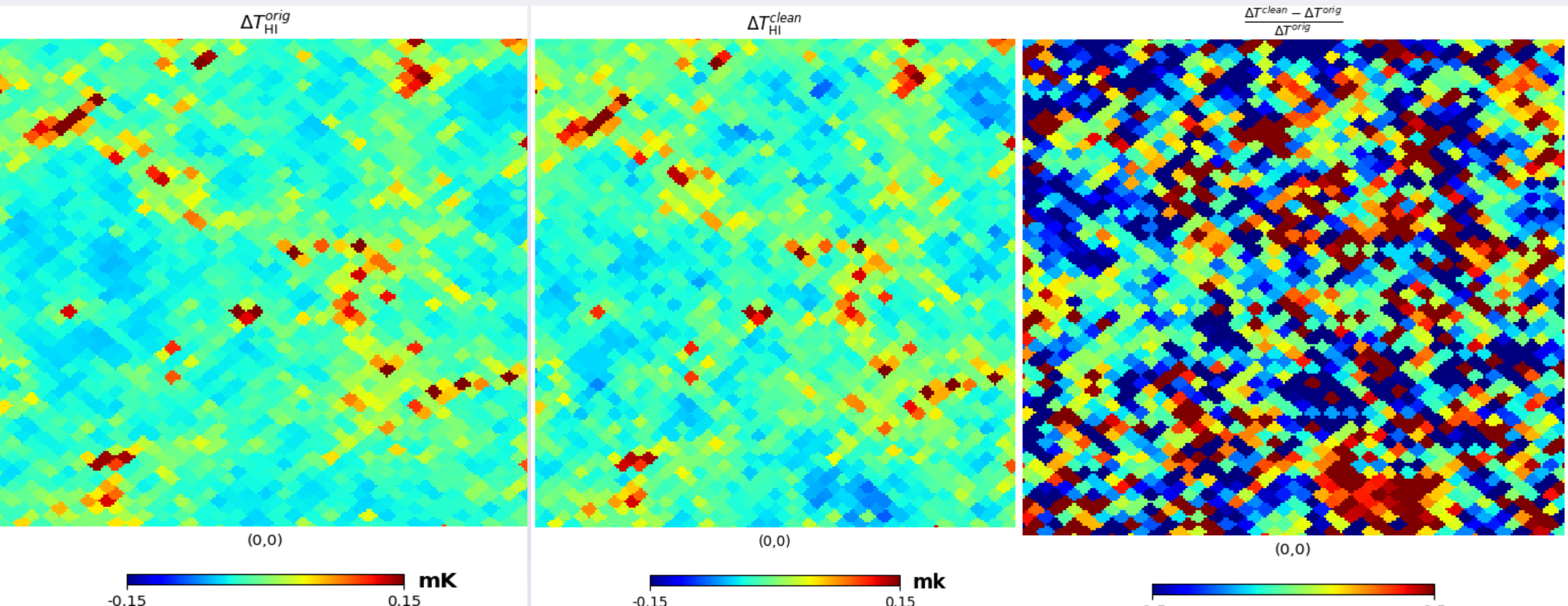

Cross power spectra

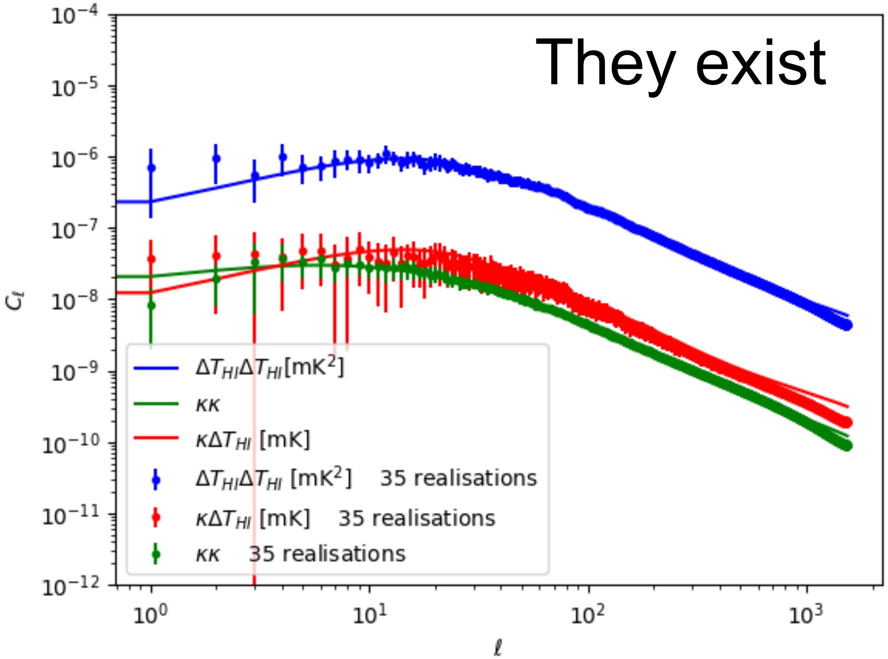

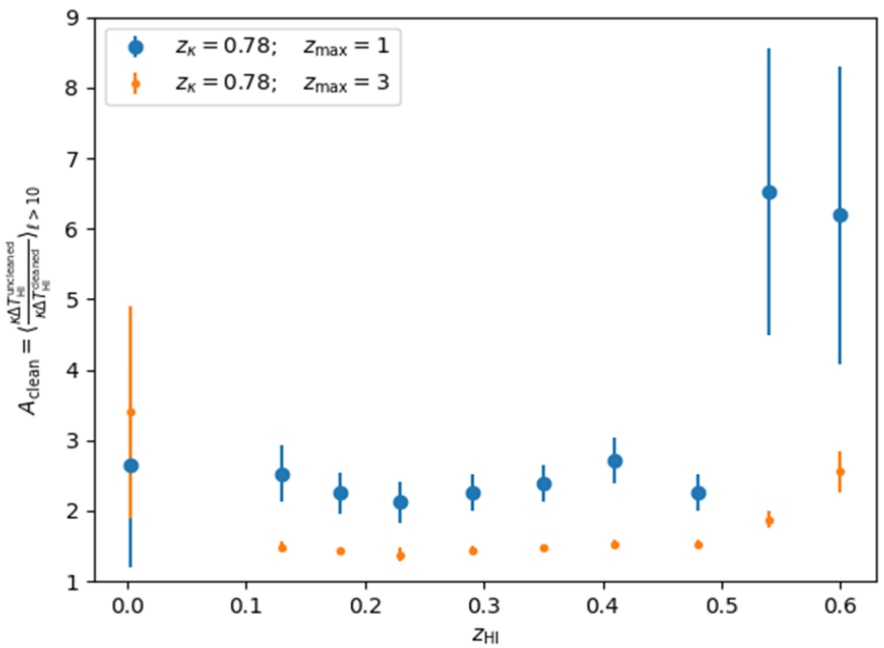

Comparison between, measured and calculated angular power spectra

$$A_{\rm clean}(z_{\rm HI}, z_\kappa, z_{\rm max}) \equiv \left\langle \frac{\kappa\Delta T_{\rm HI}^{\rm uncleaned}}{\kappa\Delta T_{\rm HI}^{\rm cleaned}} \right\rangle_{10<\ell<1500}$$

Fisher Forecast

$$\tilde{b}(z) = \alpha \times b_{\rm HI}(z)$$

$$F_{ij} \equiv \left\langle \frac{\partial^2 \mathcal{L}}{\partial\theta_i \partial\theta_j} \right\rangle$$

$$\sigma_i \geq \sqrt{F^{-1}_{ii}}$$

$$F_{ij} = \sum_{XY} \frac{\partial C^{XY^T}}{\partial\theta_i} \mathbf{COV}(C^{XY})^{-1} \frac{\partial C^{XY}}{\partial\theta_j}$$

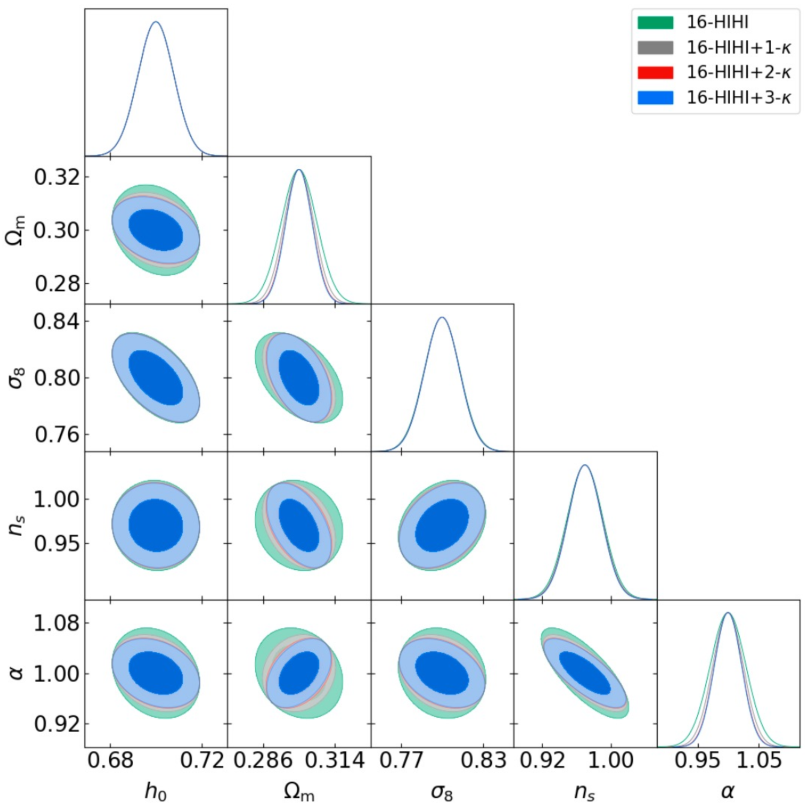

Parameters	HI bias model 1	HI bias model 2
Δh_0	0.02	0.02
$\Delta\Omega_{\rm m}$	0.01	0.02
$\Delta\sigma_8$	0.03	0.04
Δn_s	$\pm$ 0.04	$\pm$ 0.05
$\Delta\alpha$	$\pm$ 0.4	-
Δb_0	-	$\pm$ 0.04
Δb_1	-	$\pm$ 0.03

S/N single dish telescope

$$\sigma_{\rm pix} \approx \frac{T_{\rm sys}}{\varepsilon\sqrt{t_p 2\Delta\nu}} \quad T_{\rm sys} = T_{\rm rx} + T_{\rm spl} + T_{\rm CMB} + T_{\rm gal}$$

Santos et al. 2015; Seo et al. 2010

$$t_p = t_{\rm tot}(\theta_{\rm B})^2/\Omega_{\rm sur}$$

Pointing time

$$P_{\rm noise} = \sigma_{\rm pix}^2 V_{\rm pix} = r^2 y \frac{T_{\rm sys}^2 \Omega_{\rm sur}}{2\varepsilon^2 t_{\rm tot}} \quad \text{where} \quad y = cH(z)^{-1}\frac{(1+z)^2}{\nu_{21}}$$

$$S/N = \frac{P_{\rm HI}}{P_{\rm noise}}$$

MeerKAT pilot surveys

Table 3. MeerKAT pilot survey specifications (Wang et al. 2021)

$\Delta\nu$	0.2 MHz
$N_{\Delta\nu}$	[200,250]
$T_{\rm rx}$	$7.5\times10^3 + 10^3(\nu[\mathrm{MHz}]/1000 - 0.75)^2$ [mK]
$t_{\rm tot}$	10.5 hours
z	[0.3885, 0.4623]
$N_{\rm dish}$	64
$T_{\rm sys}$	16×10^3 mK
$N_{\rm pix}$	87500
$\theta_{\rm FHWM}$	1.48 deg
$\Omega_{\rm sur}$	200 deg^2

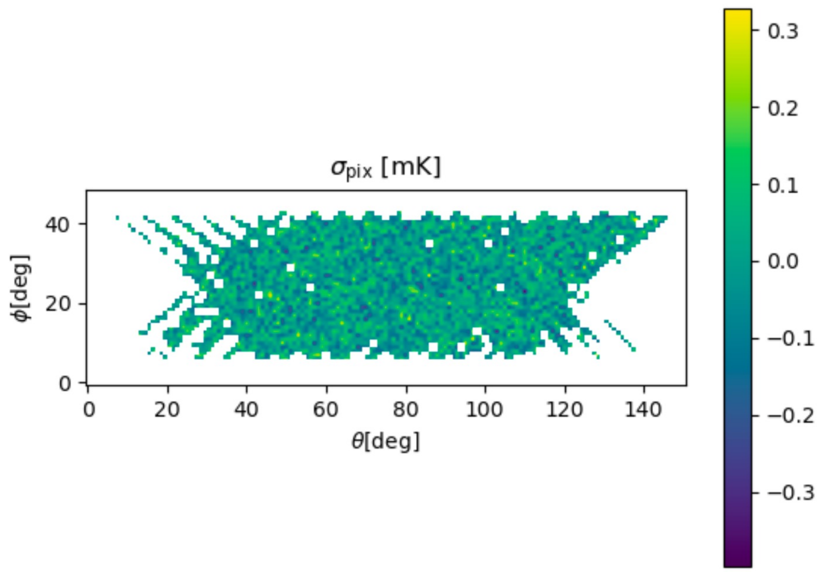

$$\sigma_{\rm pix}(\Delta\nu = 0.2) \approx 15\mathrm{mK}$$

HW: let calculate TRT's thermal noise !!!

$$973 \leq \nu \leq 1015 \text{ MHz}$$

HI intensity mapping	Maser
Pulsar search	Gravitational Physics
Pulsar Timing Array	Star formation

Is it possible to detect HI via TRT ?

Observation Mode in Cycle 0

Receiver	L-band
Frequency range	1.63 - 1.67 GHz
Polarization	Linear (Vertical)
Recording mode	Spectrometer mode for line and continuum target sources
Frequency channel resolution at max	1.907 kHz (= 0.347 km/s at 1.65 GHz)
Scanning modes	• Single-pointing • Cross-scan • Raster-scan

$\frac{S}{N}$ of $\kappa - \mathrm{HI}$

$$S/N = \frac{\sigma_{\mathrm{HI}}\sigma_{\kappa}}{\sigma_{\mathrm{T}}\sigma_{\mathrm{e}}^{n}}\sqrt{N_{\mathrm{pix}}}$$

$$S/N \approx 0.24 \quad \text{(current state of the art)}$$

Question !!!, how can we improve S/N

Instrument uncertainty study for forthcoming surveys

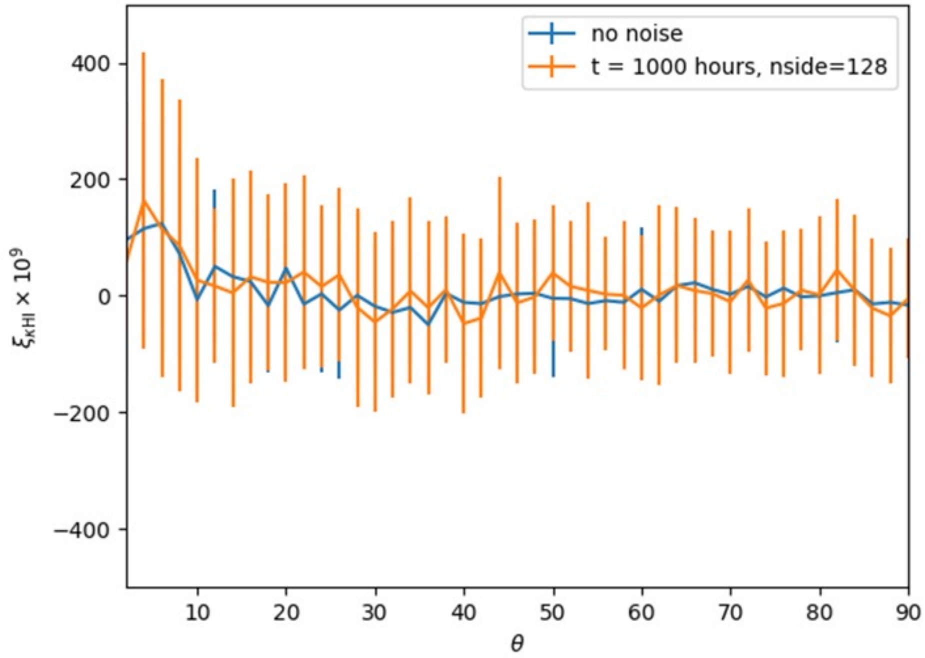

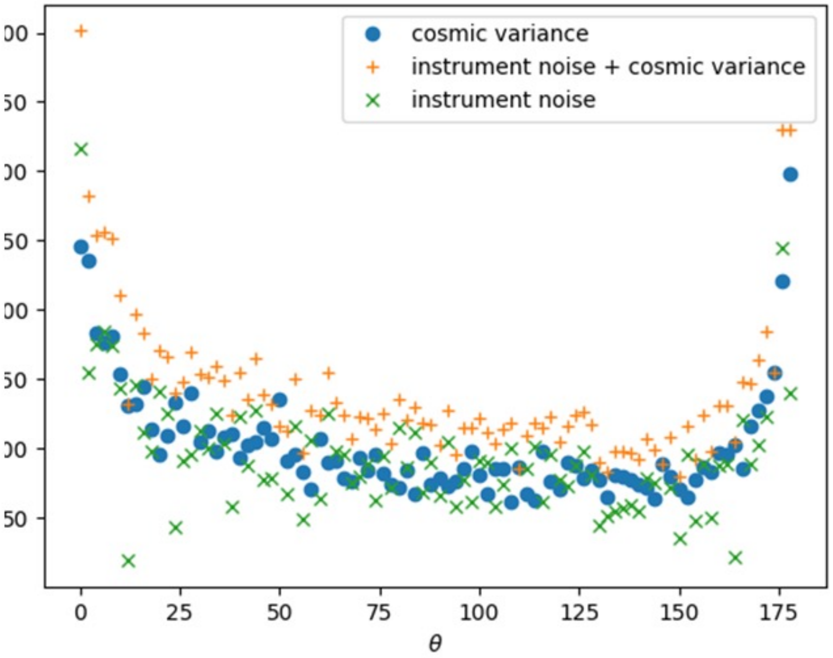

We consider the KIDs and DES for lensing and MeerKAT and GBT for HI assuming full-sky surveys + 1000hr exposure time of HI.

HI-Optical Galaxy correlation

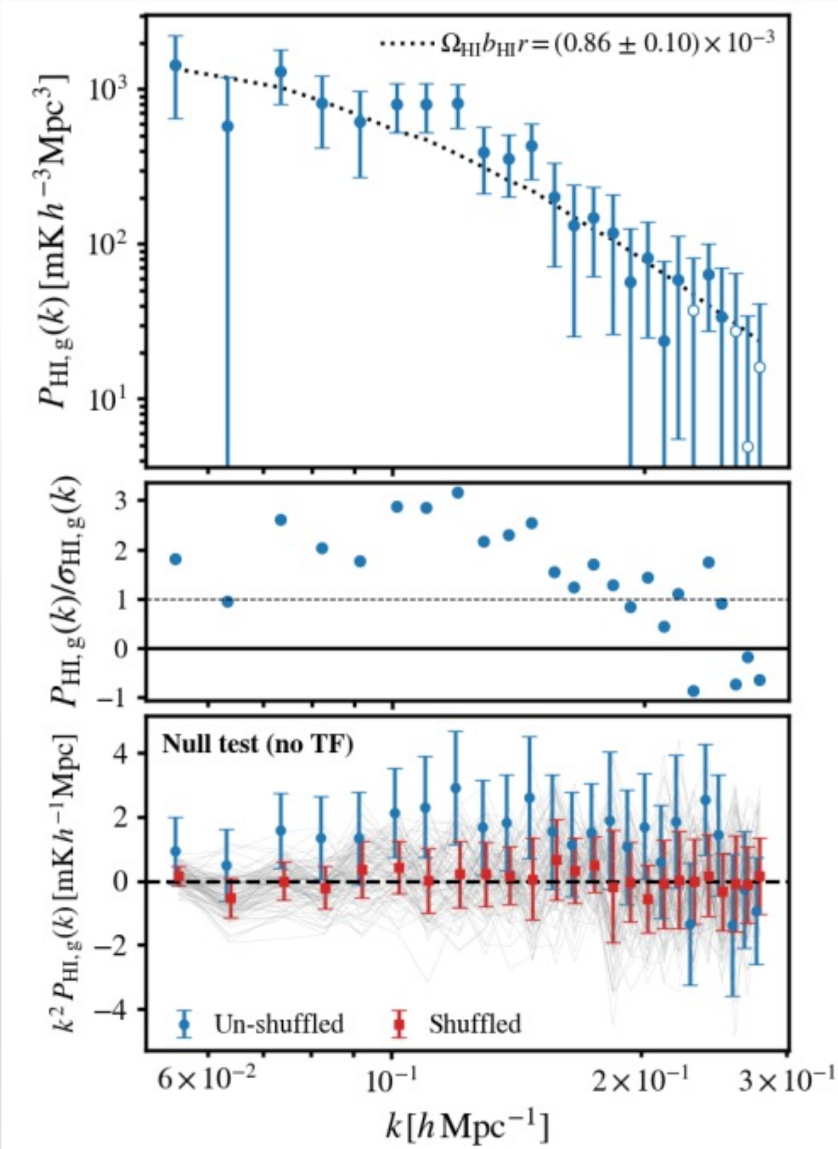

Top:MeerKAT-WiggleZ cross-power spectra by Cunnington et al. (2022); the cross-power spectra is detected at 7.7σ confidence level compared to null-test. This constraint uses the MeerKAT pilot survey (Wang et al., 2021) which has 10 hours observation time with 200 deg^{2}shared sky with WiggleZ. Middle: shows the ratio between data and error. Bottom: shows a null test where the WiggleZ galaxy maps have had been shuffled along redshift. The thin grey lines show 100 different shuffles. The average (red squares) and standard deviation (red error bars) across the shuffled samples are shown relative to the original (blue-dots). In both cases in the bottom panel, no scaling by the transfer function has been applied.

KiDs-1000 & MK pilot survey case

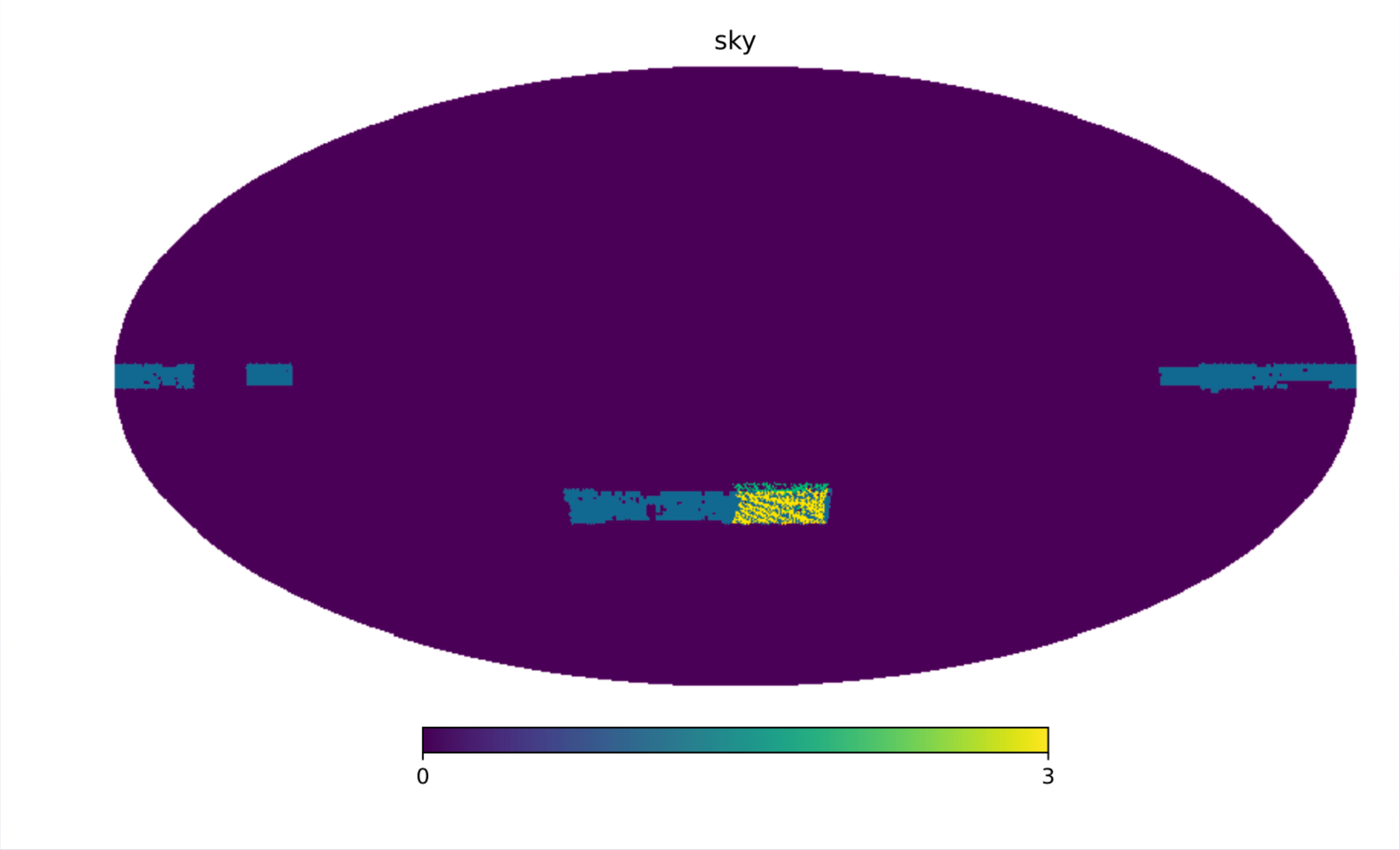

Power Spectra

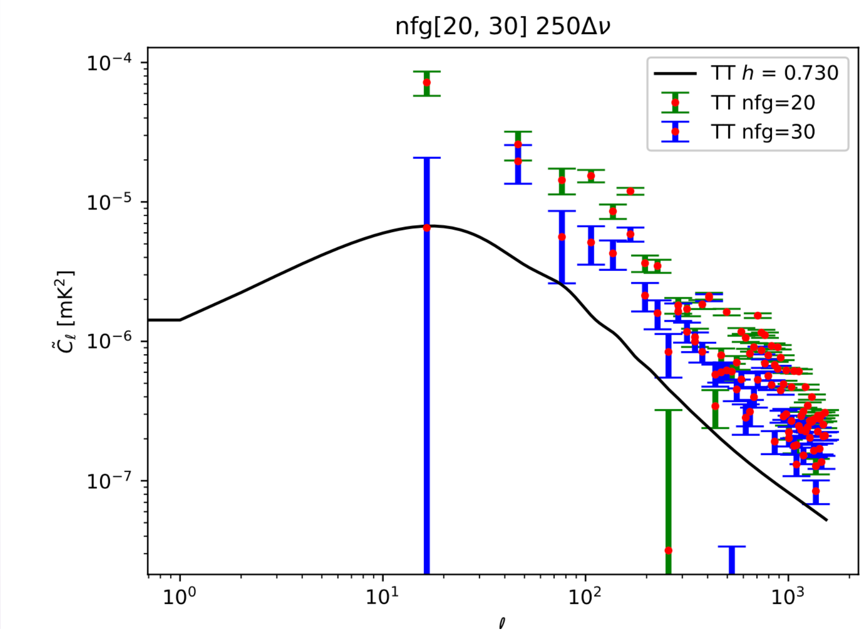

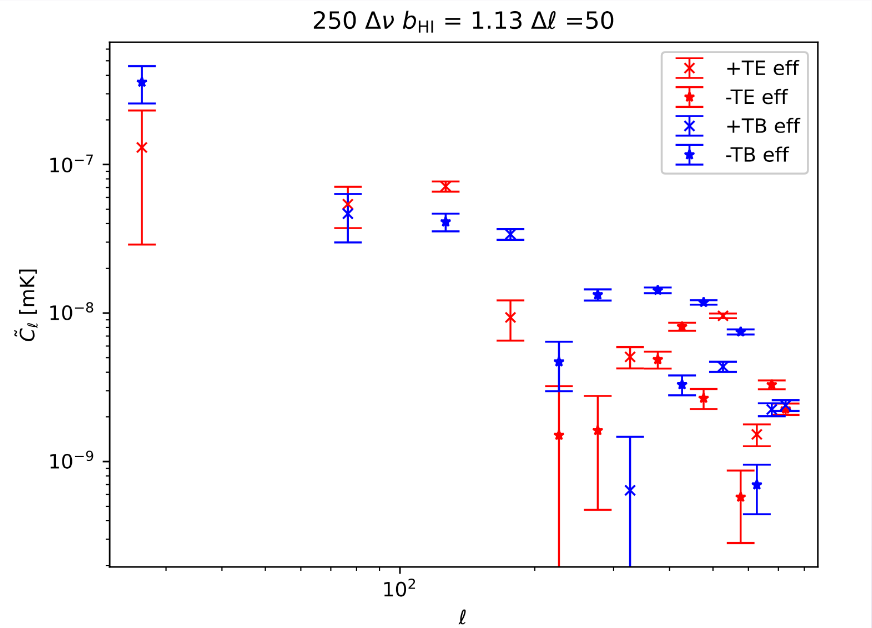

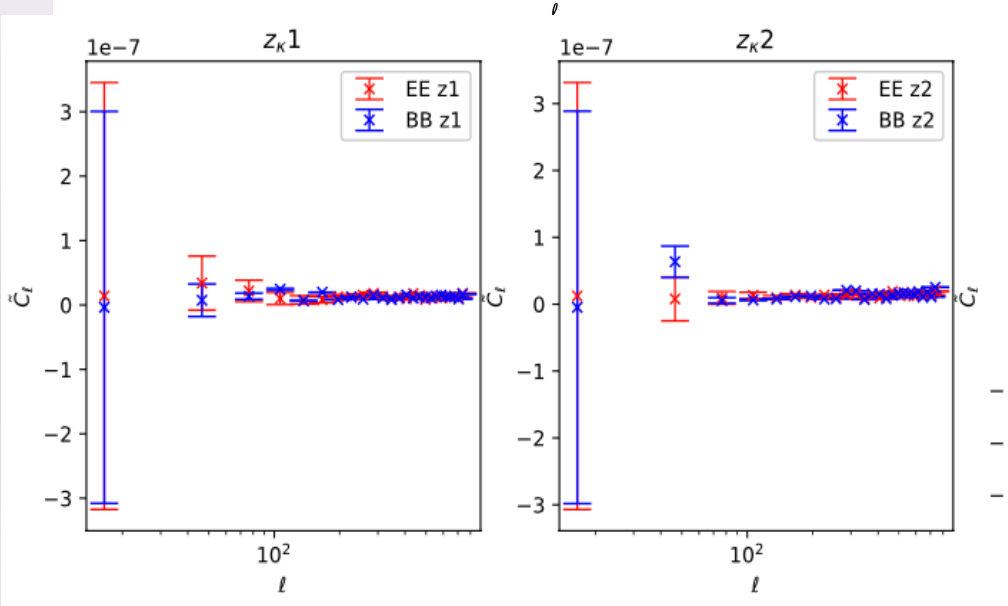

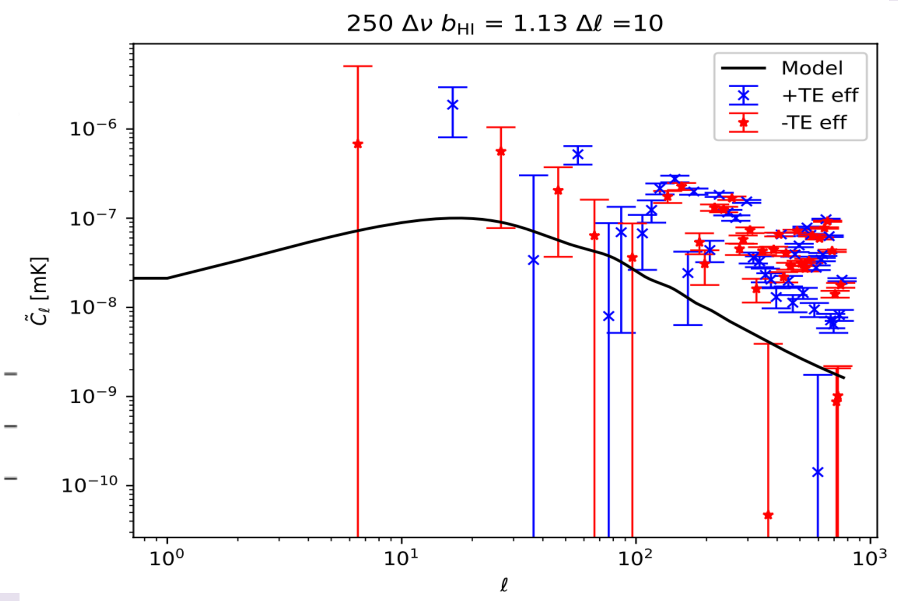

Conclusion

- The signals of cleaned cross power spectra drop by factor A_{clean}
- The cross correlations between lensing and HI can reduce the degeneracy of cosmological parameters to sufficient levels. The multiple redshift slices of HI are required for precise cosmological measurement.
- The linear evolution model of HI bias is effective enough to constrain cosmological parameters.
- Once thermal and instrument uncertainty are considered, the redshift bins size must be efficiently large enough to gain S/N
- KiDs-1000 – MK case shows that due to the small area the signal is dominated by systematic errors
- However, PCA foreground removal improves the signal especially low (l).
- We are about to detect lensing-HI correlations.

Thank You !!!